Lithos 172-173 (2013) 98–117

Contents lists available at SciVerse ScienceDirect

Lithos

journal homepage: www.elsevier.com/locate/lithos

Petrogenesis of the post-collisional volcanic rocks from the Borçka (Artvin) area: Implications for the evolution of the Eocene magmatism in the Eastern Pontides (NE Turkey)

Emre Aydınçakır [a,*], Cüneyt Şen [b]

[a] Department of Geological Engineering, Gümüşhane University, TR-29000, Gümüşhane, Turkey
[b] Department of Geological Engineering, Karadeniz Technical University, TR-61080, Trabzon, Turkey

ARTICLE INFO

Article history:
Received 4 December 2012
Accepted 3 April 2013
Available online 10 April 2013

Keywords:
Sr–Nd isotopes
Post-collisional setting
^{40}Ar–^{39}Ar geochronology
Borçka area
Eastern Pontides
NE-Turkey

ABSTRACT

Whole-rock geochemistry, ^{40}Ar–^{39}Ar data, and Sr–Nd isotopes are presented for the Eocene Borçka volcanic rocks on the eastern corner of the eastern Pontide orogenic belt (NE Turkey). Borçka (Artvin) volcanic rocks are divided into three suites—basic dyke, Borçka basalt, and Civanköy suite. These rocks contain plagioclase ($An_{49–88}$), clinopyroxene ($Wo_{38–49}En_{38–54}Fs_{8–25}$), hornblende (Mg# = 0.57–0.74) phenocrysts, and magnetite/titanomagnetite and apatite microphenocrysts. ^{40}Ar–^{39}Ar ages on hornblendes, ranging from 46.9 ± 0.1 to 39.9 ± 0.5 Ma, within the middle Eocene. The volcanic rocks show tholeiitic-calc-alkaline affinities and have low-to-medium K contents. They are enriched in large ion lithophile (LILE) and light rare earth elements (LREE), with pronounced depleted high field strength elements (HFSE). The chondrite-normalized REE patterns (La_{cn}/Lu_{cn} = 1–19) show low-to-medium enrichment, indicating similar sources for the rock suite. Initial $^{87}Sr/^{86}Sr$ values [$(^{87}Sr/^{86}Sr)_{46\ Ma}$] vary between 0.70423 and 0.70495, while initial $^{143}Nd/^{144}Nd$ values [$(^{143}Nd/^{144}Nd)_{46\ Ma}$] lie between 0.51263 and 0.51285. The main solidification processes involved in the evolution of the volcanics consist of fractional crystallization, with minor amounts of crustal contamination. All our evidences support the conclusion that the parental magma of the rocks probably derived from an enriched mantle, previously metasomatized by fluids derived from subducted slab, in a post-collisional, extension-related geodynamic setting.

1. Introduction

The Eastern Pontides form the northern margin of Anatolia, straddling the North Anatolian Transform fault, and rising steeply inland from the Black Sea coast (Fig. 1a). The Eastern Pontides represent a well-preserved arc system (Okay and Şahintürk, 1997; Şengör and Yılmaz, 1981; Yılmaz et al., 1997) resulting from the northward subduction of the Neo-Tethyan oceanic crust beneath the Eurasian plate (Fig. 1a). The Eurasian plate collided with the Tauride–Anatolide platform in the late Paleocene–early Eocene time, leading to the formation of the İzmir–Ankara–Erzincan suture (IAES) zone (Boztuğ et al., 2004; Karsli et al., 2011; Okay and Şahintürk, 1997; Şengör and Yılmaz, 1981; Topuz et al., 2011; Yılmaz et al., 1997). The Eastern Pontides are characterized by three volcanic cycles developed during the Liassic, late Cretaceous, and Eocene periods (Arslan et al., 1997; Çamur et al., 1996; Kandemir, 2004).

Eocene volcano-sedimentary and intrusive rocks cover an extensive area in Turkey (Arslan et al., 2013; Kaygusuz et al., 2011; Keskin et al., 2008; Robertson et al., 2006; Temizel and Arslan, 2009; Temizel et al., 2012; Yiğitbaş and Yılmaz, 1996), in the Caucasus (Adamia et al., 1977; Bazhenov and Burtman, 2002; Dilek et al., 2010; Vincent et al., 2005; Yılmaz et al., 2000), and in Iran (Ramezani and Tucker, 2003; Stöcklin, 1971) (Fig. 1a). In Turkey, such rocks occur on both the tectonic divide between the Pontides and the Anatolide–Tauride Block. The southern boundary of the Eocene igneous and volcano-sedimentary rocks is represented by the Bitlis–Zagros suture (BZS). Such a distribution implies that the Eocene magmatism in northern Turkey is post-collisional products with regard to the IAES, as formerly implied by Tokel (1977). Some recent models have suggested that the widespread Eocene magmatism constitutes from a (1) collisional slab break-off beneath the IAES (Altunkaynak, 2007; Boztuğ et al., 2007; Dilek et al., 2010), (2) that back-arc extensional/transtensional events related to the northward subduction along the Bitlis–Zagros suture (Robertson et al., 2006, 2007), and (3) post-collisional crustal thickening (Karsli et al., 2011; Topuz et al., 2005, 2011) and delamination of the thickened crust along the IAES (Karsli et al., 2010b; Temizel et al., 2012). In addition early Cenozoic geodynamics of the Eastern Pontides is still debated.

This study can provide important clues for understanding the petrogenetic processes of Eocene volcanic rocks in the Borçka region

* Corresponding author. Tel.: +90 4562337425; fax: +90 456 2337567.
E-mail address: emre@gumushane.edu.tr (E. Aydınçakır).

0024-4937/$ – see front matter © 2013 Elsevier B.V. All rights reserved.
http://dx.doi.org/10.1016/j.lithos.2013.04.007

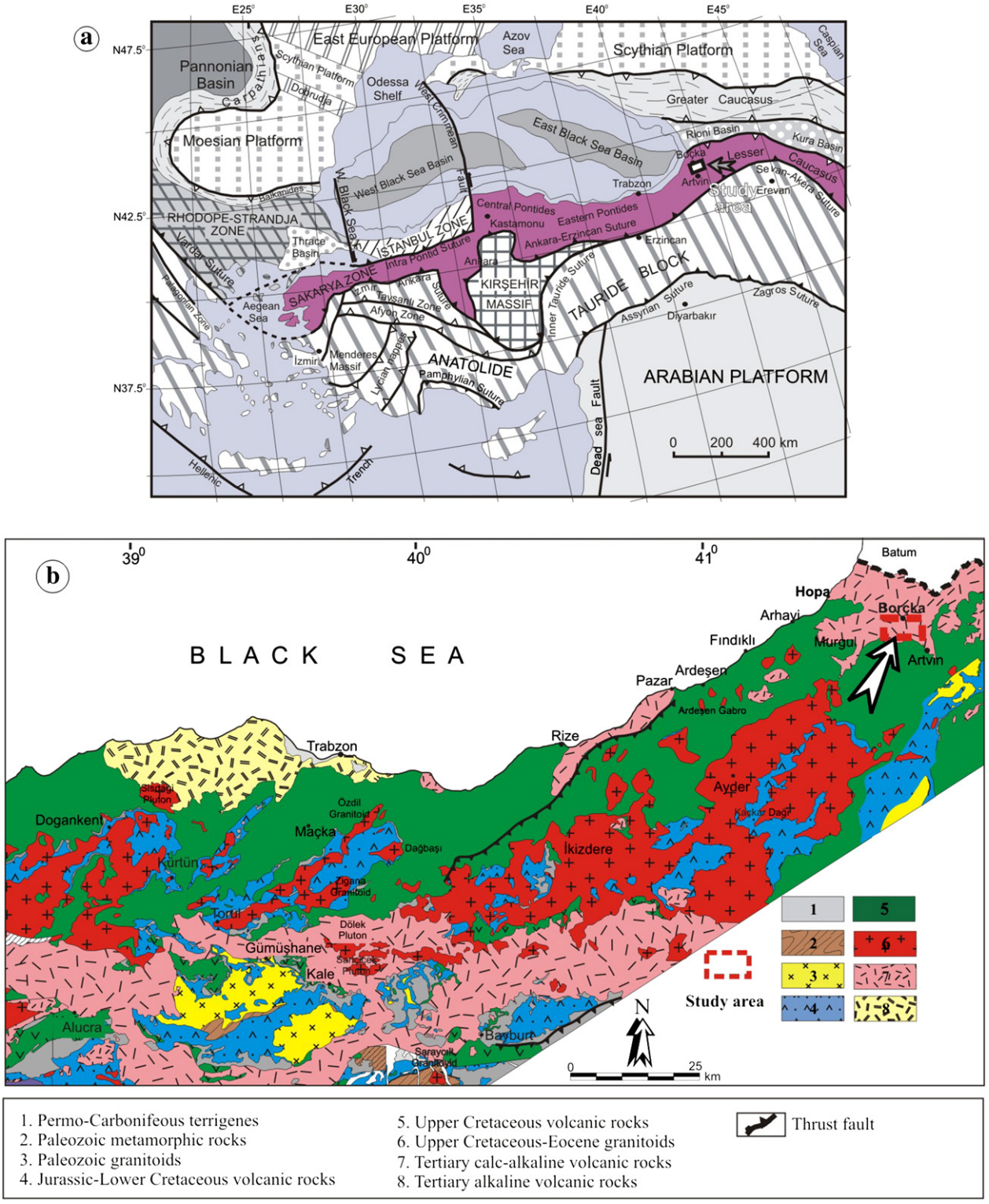

Fig. 1. a) Regional tectonic setting of Turkey with main blocks in relation to the Afro-Arabian and Eurasian plates. b) Simplified geological map of the Eastern Pontides. Panel a: modified from Okay and Tüysüz (1999); panel b: after the geological map with a scale 1:500,000; MTA (2002).

(Figs. 1 and 2). We utilize new ^{40}Ar–^{39}Ar geochronological, whole-rock geochemical, and Sr–Nd isotopic compositional data from the early Cenozoic, Borçka volcanic rocks from the northern part of the Eastern Pontides. Our objectives are to clarify the petrogenesis and tectonomagmatic evolution of the volcanic rocks in the region and to characterize the geodynamic evolution of the Eastern Pontides during the Eocene. Finally, we propose a tectono-magmatic model for generation of Borçka volcanic rocks in the Eastern Pontides, NE Turkey

2. Geological setting of the Eastern Pontides

Anatolia is made up of four major tectonic blocks or terranes that are separated by the suture zones (Okay and Tüysüz, 1999; Fig. 1a).

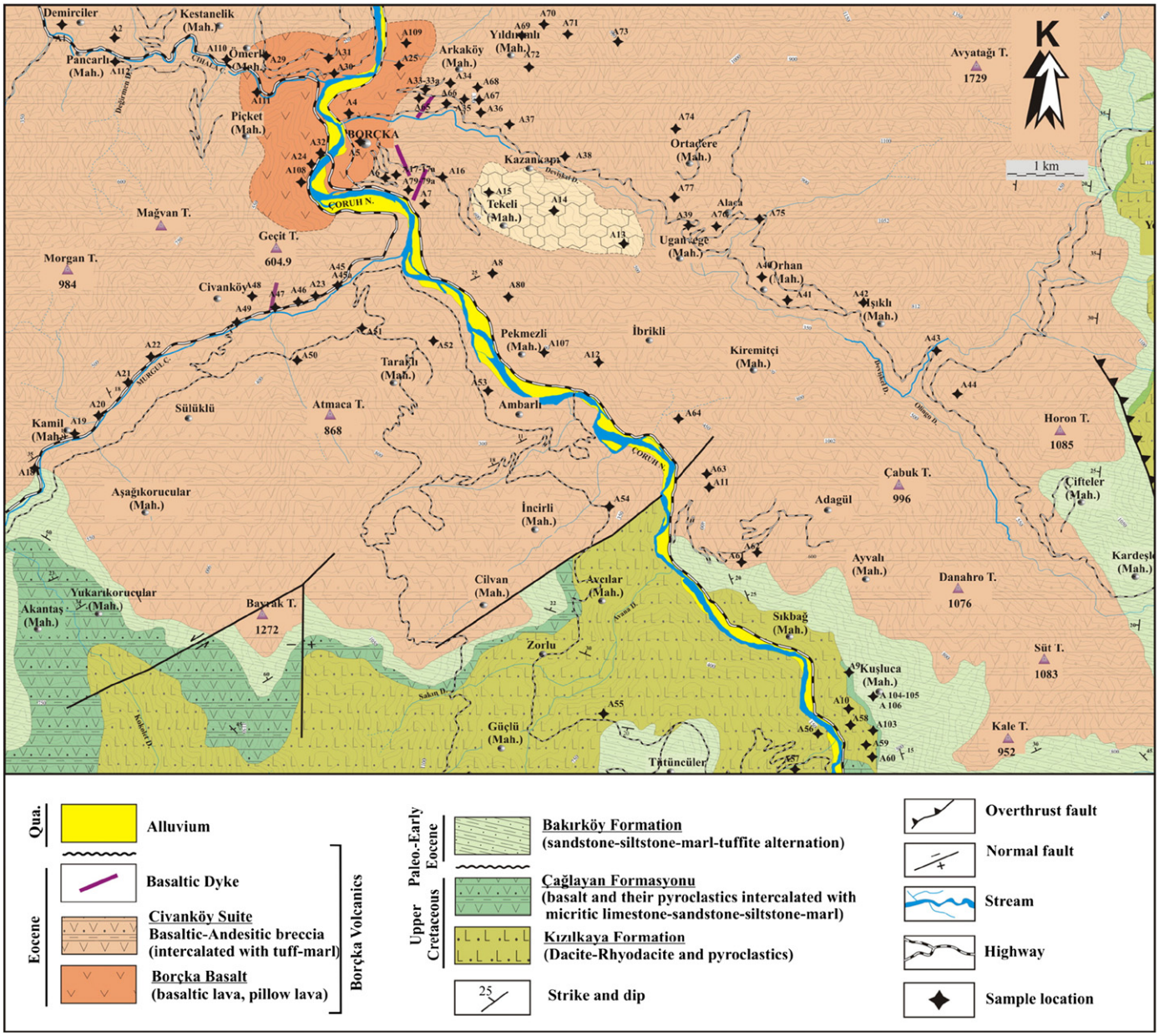

Fig. 2. Simplified geological map of the Borçka (Artvin) area.

The Eastern Pontides is a subset of the Sakarya zone, which is one of the major tectonic units of Turkey (Fig. 1a). The basement rocks of the Eastern Pontides are late Carboniferous granitoids, along with early Carboniferous metamorphic rocks (Dokuz, 2011; Kaygusuz et al., 2012; Okay, 1996; Topuz et al., 2007, 2010; Yılmaz, 1972) and late Carboniferous to early Permian, shallow marine-to-terrigenous sedimentary rocks (Çapkınoğlu, 2003; Kandemir and Lerosey-Aubril, 2011; Okay and Leven, 1996; Okay and Şahintürk, 1997; Robinson et al., 1995). The Permian and Triassic events are poorly recorded in the eastern part of the Sakarya zone due to the absence of rock formation during this time. Early Jurassic rocks were characterized by the break-up of a continental margin that rift-related volcano-sedimentary units (Dokuz and Tanyolu, 2006; Kandemir, 2004; Kandemir and Yılmaz, 2009) and basic volcanic rocks (Arslan et al., 1997; Şen, 2007) were formed. There are also late Jurassic granitoids and associated dacites that were emplaced into the Şenköy formation during the middle-late Jurassic (Dokuz et al., 2010). These granitoids are interpreted as being the products of an arc–continent collision event, in response to the closure of Paleotethys during the middle Jurassic and the accretion of the Sakarya zone to Laurasia in the north (Dokuz et al., 2010; Şengör and Yılmaz, 1981; Şengör et al., 1980; Yılmaz et al., 1997).

During the late Cretaceous, a thick unit of arc-type volcanics and intrusive rocks were emplaced into the Eastern Pontides crust in response to the northward subduction of the Neotethyan oceanic crust along the southern border of the Sakarya zone (Akın, 1979; Karsli et al., 2010a, 2012b; Okay and Şahintürk, 1999; Şengör et al., 2003; Topuz et al., 2007; Ustaömer and Robertson, 2010). The magmatic arc is represented by a more than 2 km-thick volcano-sedimentary sequence in the northern part of the Eastern Pontides, with the local intrusion of hornblende–biotite granitoids (Boztuğ and Harlavan, 2008; Boztuğ et al., 2006; Karsli et al., 2004; Kaygusuz and Aydınçakır, 2009, 2011; Kaygusuz et al., 2008; Yılmaz and Boztuğ, 1996). The southern part was in a fore-arc

phase where flyschoid sedimentary rocks with limestone olistoliths were deposited. The Paleocene period in the Eastern Pontides is attributed to a continent–continent collision between the Pontides and the Tauride–Anatolide block due to the complete closure of Neotethys. Early Cenozoic adakitic rocks, pointing to a syn- to post-collision phase, have been reported in the region (Karsli et al., 2010b, 2011; Topuz et al., 2005, 2011). The Middle Eocene time is characterized by volcanic (Arslan and Aliyazıcıoğlu, 2001; Arslan et al., 2013; Aslan, 2010; Çoban, 1997; Kaygusuz et al., 2011; Şen et al., 1998; Temizel and Arslan, 2009; Temizel et al., 2012; Tokel, 1977) and granitoids rocks (Arslan and Aslan, 2006; Karsli et al., 2007, 2012a; Yılmaz and Boztuğ, 1996) (Fig. 1b). Post Eocene terrigenous units are also observed in the area (Okay and Şahintürk, 1997). The Neogene alkaline volcanics are ascribed to post-collision extensional tectonic settings (Aydin et al., 2008, 2009).

The study area, Borçka region, is located at the east part of the Eastern Pontides in NE Turkey (Figs. 1 and 2). The main stratigraphic units in the investigated area made up of those from the late Cretaceous age, the oldest to the youngest—the Kızılkaya Formation, the Çağlayan Formation, and the Bakırköy Formation—all unconformably by Eocene-aged Borçka volcanic rocks (Fig. 2). The Kızılkaya Formation is composed of dacitic–rhyodacitic lavas and pyroclastic rocks. The Kızılkaya Formation represents the lowermost level of the study area. The Kızılkaya Formation is covered by the Çağlayan Formation in the study area. The Çağlayan Formation is composed of mainly basalt and pyroclastic, interbedded with gray-reddish micritic limestone, sandy limestone, marl, and sandstone volcano-sedimentary sequence. The age of the unit is late Santonian–Campanian or Campanian (Aydınçakır, 2012; Yılmaz et al., 1997). This unit is overlain unconformably by The Bakırköy Formation. This formation is composed of interbedded sandstone, sandy limestone, marl, and limestone. The age of the unit is Paleocene–early Eocene (Yılmaz et al., 1997). The Eocene aged part of the Borçka volcanic rocks, which rest unconformably on the late Cretaceous units, consists mainly of andesite, basalt, and associated pyroclastic rocks (tuff, breccia, and agglomerate) and pillow lavas. Basaltic lavas and breccias are outcropped in the Borçka area. Basalt lavas and breccias are dominant lithology within the sequence. Basaltic and andesitic breccias (5–35 cm in diameter) are included in the clast, ranging in size from 2 to 4 cm in diameter. The tuffs are a light brown-beige colored and medium-to-thick bedded (15–50 cm), and contain light greenish-gray and reddish marl levels. These tuffs may be classified as clastic lithic tuff. All these units are unconformably overlain by Quaternary alluvium (Fig. 2). In this study, Eocene-aged units of Borçka volcanic rocks were examined in detail.

3. Analytical methods

140 thin sections from the Borçka volcanic rocks were microscopically examined, and selected fresh samples were analyzed for mineral chemistry, whole-rock major and trace elements, Sr–Nd isotope compositions, and were dated using a ^{40}Ar–^{39}Ar laser probe technique.

3.1. Whole-rock major and trace element analyses

Thirty-three samples were selected for major and trace element analysis. To prepare the rock powders, 0.5–1 kg of the fresh samples was crushed in a steel crusher, and then, the samples were ground in an agate mill to obtain grain sizes of <200 mesh. The major and trace element contents were determined at the commercial ACME Laboratories Ltd in Vancouver, Canada. The major element oxides of the samples were measured by ICP-ES for major oxides (0.2 g pulp sample by $LiBO_2$ fusion). The detection limits are approximately 0.001–0.1 wt.%. For the trace elements, 0.2 g of the sample powder and 1.5 g of $LiBO_2$ flux were mixed in a graphite crucible and subsequently heated to 1050 °C for 15 min in a muffle furnace. The molten sample was then dissolved in 100 mL of %5 HNO_3. Sample solutions were shaken for 2 h, and then, an aliquot was poured into a polypropylene test tube and aspirated into the Perkin-Elmer Elan 600 ICP mass spectrometer. Calibration and verification standards (STD SO 18), together with reagent blanks, were added to the sample sequence. The detection limits determine the range from 0.01 to 0.5 ppm for most trace elements.

3.2. Microprobe analyses

Mineral compositions were determined on a polished thin section using a Cameca SX-100 electron microprobe at the Institute of Mineralogy and Petrology in Hamburg University (Germany), equipped with five wavelength-dispersive spectrometers. The analytical conditions were 15 kV accelerating voltage, 20 nA beam current, and 20 s counting time.

3.3. Sr–Nd isotope analyses

Nd and Sr isotope analyses were conducted at the Institute of Geology and Geophysics, Chinese Academy of Sciences (Beijing). Samples were dissolved using acid ($HF + HClO_4$) in sealed Savillex beakers on a hot plate for one week. The separation of Rb, Sr, and light REE was achieved through a cation-exchange column (packed with BioRad AG 50W-X8 resin). Sm and Nd were further purified using a second cation-exchange column that was conditioned and eluted with diluted HCl. Mass analyses were conducted using a multi-collector VG354 mass spectrometer, as described by Qiao (1988). $^{87}Sr/^{86}Sr$ and $^{143}Nd/^{144}Nd$ ratios were corrected for mass fractionation relative to $^{86}Sr/^{88}Sr = 0.1194$ and $^{146}Nd/^{144}Nd = 0.7219$, respectively. Finally, the $^{87}Sr/^{86}Sr$ ratios were adjusted to the NBS-987 Sr standard = 0.710250, and the $^{143}Nd/^{144}Nd$ ratios to the La Jolla Nd standard = 0.511860. The uncertainties in concentration analyses by isotopic dilution are 2% for Rb, 0.5% for Sr, and 0.2–0.5% for Sm and Nd, depending upon the concentration levels. Procedural blanks are: Rb = 80 pg, Sr = 300 pg, Sm = 50 pg, and Nd = 50–100 pg. The detailed explanation of sample preparation, errors, and analytical precision is provided in Zhang et al. (2002).

3.4. ^{40}Ar–^{39}Ar dating

Hornblende grains were separated from the Borçka volcanic rocks for ^{40}Ar–^{39}Ar dating. The samples were crushed and the 80–100 μm size fractions were separated. Approximately 2 mg of hornblende was packaged in pure aluminum foil for each sample (in duplicate). The foil packets were placed in evacuated quartz tubes and irradiated in the 49-2 nuclear reactor at the Institute of Chinese Atomic Energy (48 h 06 m). Neutron flux variation (J) was measured using the standard mineral, Zhoukoudian biotite (ZBH-25, Age:132 Ma). All age estimates include uncertainties at the value of (J). After irradiation, the sample packets were opened and the hornblende placed into 2 mm-diameter wells in a copper disk and heated to total fusion using the New Wave Research CO_2 laser instrument connected to a GV 5400 Noble Gas MS at Peking University. The extraction Line (Zr–Al) is similar to the equipment used in the Berkeley Geochronology Center; measurements were performed on an automatic ^{40}Ar–^{39}Ar laser-probe dating system, with multiple grain fusions analyzed. The details of the Ar isotope analyses are similar to those reported by Hall and Farrell (1995). All analyses were corrected for fusion-system blank levels at the five Ar mass positions: blanks were run for every three analyses. Blank levels were approximately 3.9×10^{-16} mol at ^{40}Ar and 1.8×10^{-17} mol at ^{36}Ar. Data processing was similar to that described by Nomade et al. (2005).

4. Results

4.1. Petrography and mineral composition

The Eocene aged units of the Borçka volcanic rocks studied are mainly Borçka basalt (basaltic lava and pillow lava), Civanköy suite (basaltic–andesitic breccia and tuff), and basaltic dyke. They show porphyric, microlitic–porphyric, hyalo-microlitic porphyric, hyalopilitic, poikilitic, glomeroporphyric and rarely intersertal, intergranular, and fluidal textures (Fig. 3).

The Borçka basaltic rocks were examined in terms of their textures and mineralogical compositions. Typical mineral assemblages

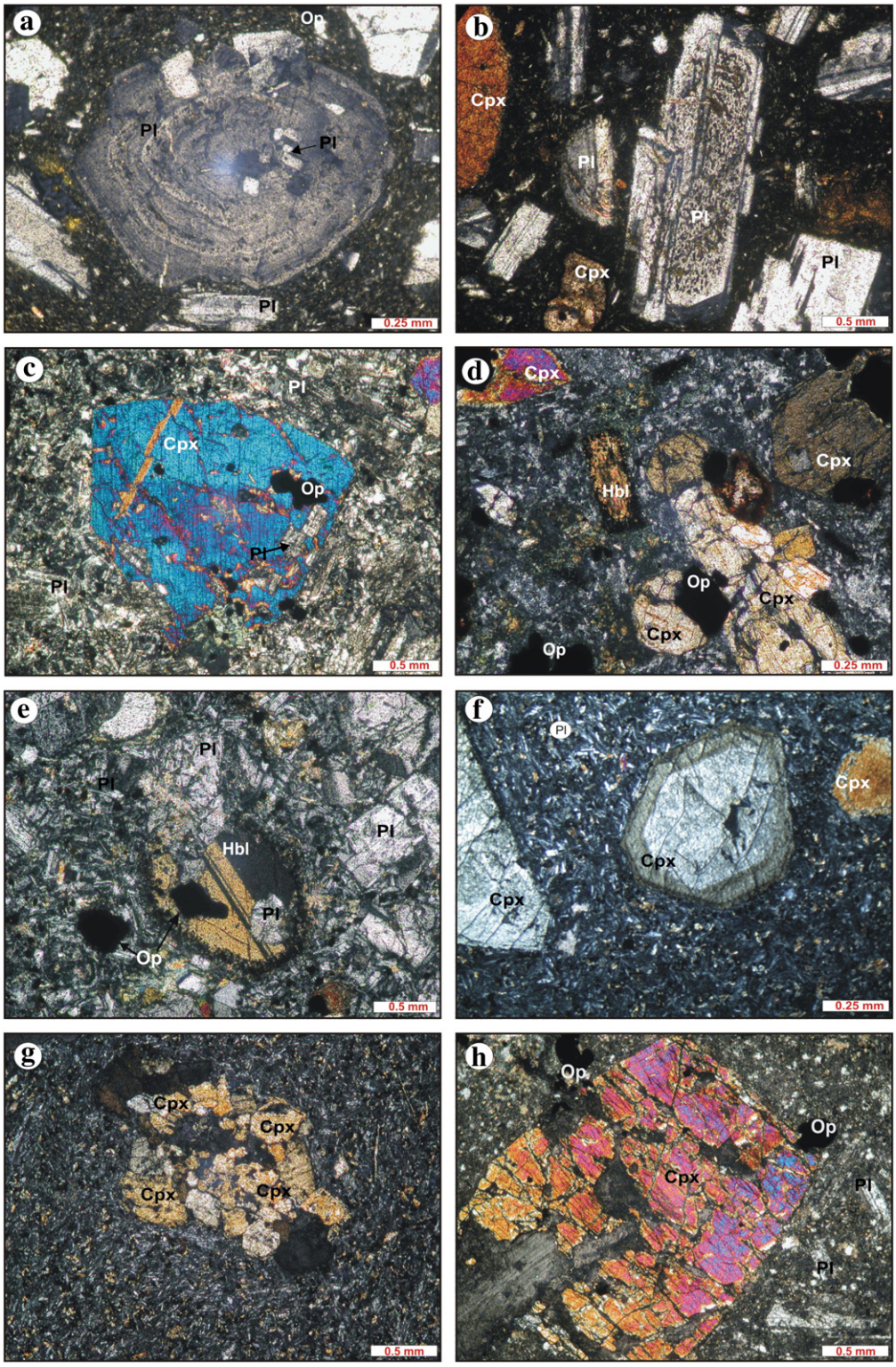

Fig. 3. Photomicrograph showing textural relationships of the volcanics. The features are clinopyroxene (Cpx), hornblende (Hbl), plagioclase (Pl), opaque (Op).

in the rocks are plagioclase, clinopyroxene, hornblende, and Fe–Ti oxide. Plagioclases range from labradorite to bytownite (Fig. 4a and Supplementary Table 1) in composition (An_{64-87}), occur mainly as euhedral-to-subhedral crystals, and are present both as phenocrysts and microlites in the glassy-fluidal groundmass (Fig. 3a). Plagioclases also exhibit albite twinning and oscillatory zoning. Clinopyroxenes ($Wo_{38-47}En_{38-54}Fs_{10-18}$) are euhedral-to-subhedral grains, and are diopside-augite (Morimoto, 1988; Fig. 4b; Supplementary Table 1). Hornblende (Mg# = 0.83–0.96) occurs as euhedral-to-subhedral crystals, and are magnesio-hastingsite (Fig. 4c; Supplementary Table 1) in composition based on nomenclature of Leake et al. (1997). Hornblende is, in many cases, characterized by opaque rims and chloritization (Fig 3d). The Fe–Ti oxides are magnetite–titanomagnetite (Supplementary Table 1). The groundmass is composed of subhedral plagioclase microlites and glass.

The Civanköy Suite—basaltic–andesitic breccias—consists mainly of plagioclase, hornblende, clinopyroxene, and Fe–Ti oxide (Fig. 3b, d). Plagioclases (An_{49-88}) (Fig. 4a and Supplementary Table 1), with euhedral-to-subhedral crystals, are present, both as phenocrysts and microlites in the groundmass. Some of these show sieve-textured and oscillatory zoning (Fig. 3a, b). Clinopyroxene ($Wo_{46-47}En_{40-42}Fs_{12-14}$) phenocrysts are diopside-augite (Fig. 4b and Supplementary Table 1). Clinopyroxene phenocrysts display twinning and contain inclusions of plagioclase and opaque minerals (Fig. 3c). Hornblende occurs as both subhedral and euhedral grains, and is classified (Leake et al., 1997) as magnesio-hastingsite (Mg# = 0.81–0.90) (Fig. 4c and Supplementary Table 1). Hornblendes are characterized by opaque rims and are also corroded (Fig. 3e). Some of them include Fe–Ti oxide and plagioclase, and show chloritization (Fig. 3e). Fe–Ti oxides are titanomagnetite (Supplementary Table 1). The groundmass is composed of lath-shaped plagioclase microlites, augite and opaque minerals, and rare glass.

The basaltic dykes consist of plagioclase, clinopyroxene, and Fe–Ti oxide. Plagioclases are bytownite (An_{84-87}), and occur mainly as subhedral laths and microlites in the groundmass (Fig. 4a and Supplementary Table 1). Clinopyroxenes ($Wo_{46-48}En_{35-43}Fs_{9-17}$) are diopside-augites (Fig. 4b). The Cpx typically shows oscillatory zoning (Fig. 3f). Oxides are magnetite in the basaltic dyke (Supplementary Table 1). The groundmass is microcrystalline and consists of plagioclase microlites, clinopyroxene grains, and glass.

4.2. ^{40}Ar–^{39}Ar dating

The ^{40}Ar–^{39}Ar age determination on the hornblende separates of the three volcanic samples are presented in Supplementary Table 2. The hornblende separates yield ages of 46.1 ± 0.6 Ma for the basaltic andesite lava flows, 46.0 ± 0.8 Ma for the basaltic lava flow, and 39.9 ± 0.5 Ma for the andesitic lava flow (Fig. 5), corresponding to the middle Eocene.

4.3. Major and trace elements

Major oxides and trace element data are given in Table 1. The volcanic rocks from the Borçka area display a large compositional spread, with SiO_2 contents ranging from 42 to 63 wt.% and Mg# values range from 21 to 41 (Table 1). In the total alkali–silica diagram (Fig. 6a), the Borçka volcanics fall into the fields of basalt, basaltic andesite, andesite, dacites, trachy-basalt, and basaltic trachy-andesite.

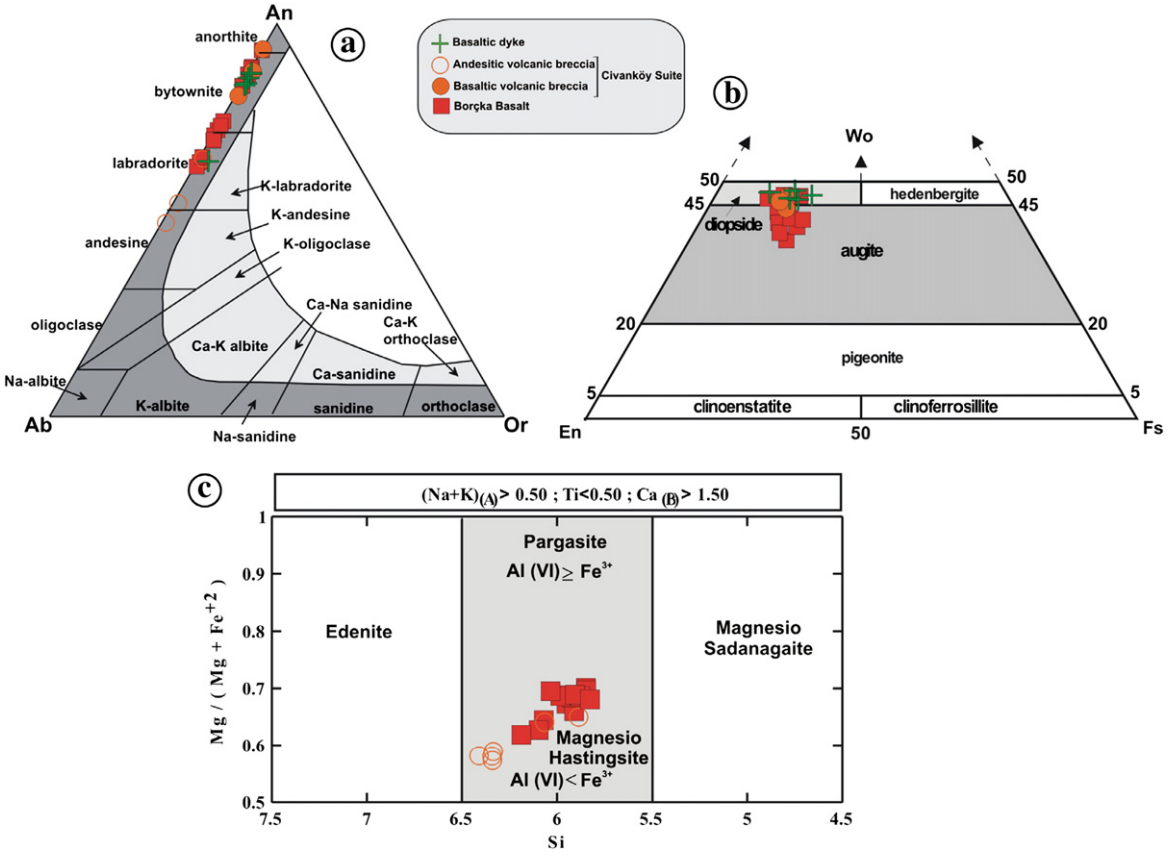

Fig. 4. (a) An–Ab–Or triangular plot showing the compositions of feldspars in the Borçka volcanic rocks, (b) clinopyroxene classification diagram (Morimoto, 1988) of the Borçka volcanics, and (c) hornblende classification diagram (Leake et al., 1997) of the Borçka volcanic rocks.

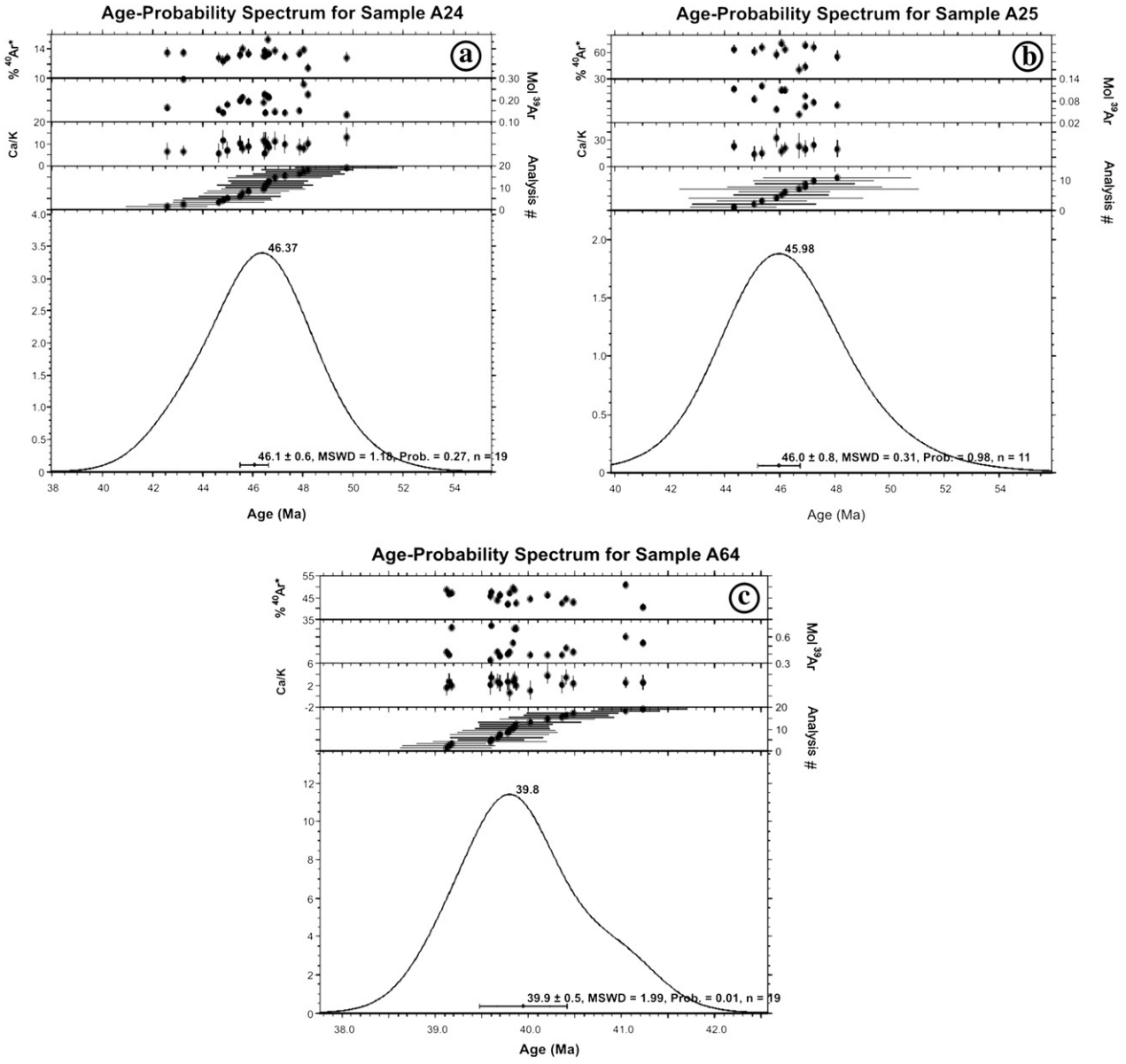

Fig. 5. ^{40}Ar–^{39}Ar age-probability distributions for the three irradiations.

In the Zr/TiO_2*0.0001 versus Nb/Y diagram (Winchester and Floyd, 1977), which uses only relatively immobile elements, the studied volcanic rocks plot in the fields of andesite/basalt, andesite, rhyodacite/dacites, and one sample in trachy-andesite (Fig. 6b). On a K_2O versus Na_2O diagram (Le Maitre, 2002), basaltic dyke samples plot into the low-K area, and the basaltic lava and basaltic–andesitic volcanic breccia samples show a tendency of the low-K and medium-K area (Fig. 6c). However, in an AFM diagram (Fig. 6d), all the samples display tholeiitic-calc-alkaline trend.

Harker variation diagrams show chemical trends, which are consistent with fractional crystallization. The analyzed samples generally exhibited negative correlations between SiO_2 and CaO, MgO, $Fe_2O_3^{tot}$, TiO_2, Ni, and Co and positive correlations between SiO_2 and K_2O, Na_2O, Al_2O_3, P_2O_5, Sr, Ba, Zr, Nb, and Th, respectively (Fig. 7). All these variations can be explained by the fractionation of common mineral phases such as clinopyroxene ± hornblende ± plagioclase ± magnetite ± apatite in volcanic rocks.

The studied Borçka volcanic rocks display variable enrichment in large ion lithophile elements (LILE), high field strength elements (HFSE), light rare earth elements (LREE), and heavy rare earth elements (HREE) with respect to primitive mantle and chondrite (Fig. 8a, b). Primitive mantle-normalized (Sun and McDonough, 1989) trace element patterns show similar enrichments in large ion lithophile elements (LILE; Ba, Rb, Th and K), Th and Ce, and depletions in some high field strength elements (HFSE; Zr, Y, Nb and Ti) (Fig. 8a).

Chondrite-normalized (Boynton, 1984) REE patterns (Fig. 8b) are enriched in LREE, relative to HREE. All volcanic rocks (basaltic dyke, pillow lava basalt, basaltic lava, and basaltic–andesitic volcanic breccia) show moderately fractionated chondrite-normalized REE patterns, parallel to each other with La_N/Lu_N = 2–20, indicating a similar or the same source region for the Borçka volcanic rocks. All volcanic rocks show slight and no Eu (mean Eu_N/Eu^* =0.93–1.18) anomalies (Fig. 8b), suggesting insignificant plagioclase fractionation.

4.4. Sr–Nd isotopes

The Sr–Nd isotopic compositions of selected samples from the Borçka volcanic rocks are listed in Table 2 and plotted in Fig. 9. All the samples show a small range of Sr–Nd isotope ratios with initial $^{87}Sr/^{86}Sr$ values

Table 1
Whole-rock analyses of selected samples from the Borçka volcanic rocks. $Fe_2O_3^{tot}$, total iron as Fe_2O_3. LOI: loss on ignition. Mg# (Mg-number) = 100 × MgO/(MgO+$Fe_2O_3^{tot}$). Oxides are given in wt.%, trace elements in ppm.

Rock type	Basaltic dyke		Borçka basalt															
Samples	A17A	A79A	A15	A113	A1	A2	A5	A14	A16	A24	A25	A29	A38	A73	A109	A110	A111	A112
SiO_2	43.47	43.93	51.08	41.63	51.23	51.22	50.71	51.37	45.67	52.61	46.11	51.63	48.66	48.79	45.87	47.09	53.44	50.24
TiO_2	0.71	0.71	0.59	0.71	0.58	0.69	0.69	0.68	0.75	0.54	0.74	0.66	0.71	0.90	0.79	0.65	0.56	0.68
Al_2O_3	15.74	15.46	20.26	17.48	18.90	18.51	17.76	18.11	17.41	17.75	18.15	18.61	19.39	17.92	18.09	18.28	18.35	18.68
$Fe_2O_3^{tot}$	10.71	10.91	7.47	10.40	8.37	9.79	9.02	9.33	10.96	9.06	10.31	9.20	10.52	9.48	10.61	10.19	7.96	9.98
MnO	0.19	0.18	0.10	0.16	0.18	0.30	0.15	0.18	0.19	0.19	0.18	0.23	0.18	0.18	0.17	0.22	0.19	0.20
MgO	9.45	9.04	3.09	6.61	4.00	4.47	5.51	4.54	7.30	4.23	7.21	3.96	4.93	4.94	6.94	5.77	3.12	4.38
CaO	11.75	11.53	7.83	11.04	8.52	8.94	9.67	8.33	11.65	9.03	11.94	10.03	8.42	11.16	11.80	9.40	8.29	8.55
Na_2O	1.75	1.72	3.31	2.15	3.71	2.39	2.46	2.89	1.91	2.64	1.72	2.29	4.52	2.74	1.78	2.62	2.89	2.81
K_2O	0.10	0.10	0.72	1.38	0.34	0.38	0.22	1.73	0.73	0.73	0.60	0.43	0.87	0.26	0.51	0.17	0.97	0.64
P_2O_5	0.18	0.19	0.13	0.13	0.13	0.11	0.13	0.18	0.09	0.14	0.08	0.18	0.29	0.21	0.09	0.06	0.18	0.13
LOI	5.6	5.8	5.2	8.0	3.9	3.0	3.4	2.4	3.1	2.8	2.7	2.5	1.2	3.2	3.0	5.3	3.8	3.5
Total	99.71	99.65	99.81	99.72	99.81	99.82	99.78	99.73	99.73	99.76	99.74	99.74	99.74	99.76	99.69	99.78	99.77	99.78
Ni	83.2	74.6	1.5	23.4	5.2	4.4	14.7	6.7	19.3	8.6	17	3.3	4.1	10.1	16.8	5.1	5.3	3.4
Sc	53	50	18	46	20	24	34	27	44	22	48	21	24	31	48	30	15	24
Ba	87	81	214	149	254	216	276	729	357	390	330	336	283	256	310	69	453	202
Co	44	46	17.7	36.7	19.6	25.3	26.1	23.8	33.8	22.1	33.6	19.7	25.1	27.1	34.6	22.5	10.6	23.8
Cs	0.1	<0.1	0.3	2.9	0.2	0.4	<0.1	0.6	<0.1	0.1	<0.1	0.7	1.3	<0.1	<0.1	0.1	1	0.6
Ga	14.4	16	16.4	13	16.1	16.5	15.3	15.8	14.4	16.5	14.9	17.2	16.1	17.4	14.8	16	16.1	17.2
Hf	0.9	0.8	1.6	0.6	1.8	1.4	1.4	1.7	0.8	1.1	0.7	1.2	1.4	1.7	0.9	0.9	1.2	1.1
Nb	1.4	1.4	1.5	0.7	1.9	1.4	1.4	1.5	0.9	1.2	1.8	1.3	1.6	2.1	0.7	0.9	1.4	1.4
Rb	0.9	1.3	9.6	28.4	5.8	6.6	2	31.1	9.7	15.5	6.3	8.9	18.9	1.3	5.6	2.5	20.1	13.1
Sr	389	414.5	333.8	487.8	402	282.2	471.2	502.4	378.9	466.9	349.8	520.5	524.7	476.9	346.3	271.5	481.1	302
Ta	<0.1	<0.1	<0.1	<0.1	<0.1	<0.1	<0.1	<0.1	<0.1	<0.1	0.2	<0.1	<0.1	0.2	<0.1	<0.1	<0.1	<0.1
Th	2.2	2.5	0.8	0.8	1.1	0.5	1.5	2	1	1.1	0.7	1.1	2.1	1.8	0.5	0.4	1.1	0.6
U	0.6	0.7	0.3	0.2	0.4	0.2	0.6	0.8	0.4	0.5	0.2	0.5	0.5	0.6	0.2	0.2	0.5	0.2
V	372	389	180	330	205	253	302	276	349	209	339	220	254	292	358	260	146	255
Zr	35.7	32.6	44.8	20.9	59.7	38.7	41.5	53.9	30.5	41.5	25.7	38.4	44.4	62.8	22.1	31.6	45.3	37.1
Y	10.9	11.3	15.5	8.5	16.2	15.4	14.7	16.3	11.2	14.3	11.6	16	15.6	20.8	11.9	12.5	15.4	15.4
Cu	79.1	73.8	36.1	70.7	35.2	28.1	62.9	63.8	77.6	36.4	70.9	23.3	14.8	121.1	72.4	38.8	14.3	25.9
Pb	2.2	163	1.7	2.1	3.6	1.4	3.7	6.3	3.2	5.4	2.7	1.5	3.6	5	3.2	1.2	8.8	1.1
Zn	56	133	36	49	58	58	50	46	44	64	45	42	48	45	46	50	39	31
La	9.4	9.7	5.1	4.5	5.8	5.8	7.6	10.1	4.2	5.6	2.7	6.1	7.8	9.5	3.1	3.1	6.3	4.2
Ce	19.6	19.5	11.9	10.5	11.8	12.8	14.2	19.7	8.9	12	6.3	13.5	16.8	21.8	6.8	7.1	14.3	10.6
Pr	2.58	2.67	1.6	1.42	1.67	1.8	1.96	2.69	1.27	1.68	0.99	1.89	2.32	3.03	1.09	1.05	1.95	1.52
Nd	11.2	10.5	7.5	6.8	7.6	8.5	8.5	11.8	5.9	7.4	5.5	8.3	10.8	13.8	6.2	5.1	9.4	7.6
Sm	2.54	2.69	1.95	1.67	1.96	2.03	2.08	2.83	1.54	1.98	1.48	2.26	2.59	3.36	1.58	1.46	2.37	2.05
Eu	0.85	0.88	0.77	0.63	0.76	0.79	0.78	0.96	0.64	0.79	0.61	0.91	0.9	1.15	0.63	0.64	0.92	0.79
Gd	2.49	2.47	2.46	1.74	2.33	2.39	2.43	3	1.89	2.13	1.79	2.56	2.67	3.62	2.05	1.89	2.56	2.44
Tb	0.39	0.39	0.43	0.29	0.43	0.43	0.42	0.48	0.33	0.42	0.32	0.5	0.49	0.6	0.37	0.36	0.43	0.43
Dy	2.11	2.2	2.6	1.47	2.64	2.51	2.52	2.75	1.98	2.55	1.96	2.68	2.71	3.48	2.22	2.07	2.41	2.51
Ho	0.4	0.37	0.58	0.3	0.57	0.54	0.53	0.57	0.42	0.54	0.44	0.66	0.61	0.73	0.46	0.43	0.55	0.53
Er	1.13	1.13	1.71	0.97	1.74	1.71	1.62	1.77	1.18	1.63	1.23	1.68	1.66	2.16	1.32	1.39	1.63	1.69
Tm	0.18	0.2	0.25	0.14	0.28	0.27	0.25	0.27	0.19	0.29	0.2	0.32	0.3	0.33	0.21	0.23	0.27	0.26
Yb	1.05	1.07	1.75	0.83	1.82	1.65	1.53	1.74	1.23	1.59	1.17	1.77	1.63	2.08	1.27	1.5	1.57	1.53
Lu	0.15	0.16	0.27	0.13	0.28	0.26	0.24	0.27	0.17	0.28	0.17	0.31	0.29	0.31	0.19	0.23	0.25	0.26
EuN/Eu*	1.02	1.03	1.07	1.12	1.09	1.09	1.06	1.00	1.15	1.17	1.14	1.15	1.04	1.00	1.07	1.18	1.14	1.08
LaN/YbN	6.05	6.13	1.97	3.66	2.15	2.38	3.36	3.92	2.31	2.38	1.56	2.33	3.23	3.09	1.65	1.40	2.71	1.85
Mg#	47	45	39	29	32	31	38	33	40	32	41	30	32	34	40	36	28	31

[($^{87}Sr/^{86}Sr)_{46}$] ranging from 0.70423 to 0.70495 and ($^{143}Nd/^{144}Nd)_{46}$ ratios (0.51263–0.51285) corresponding to ε_{Nd} from 0.5 to 5.1. The Nd model ages (T_{DM}) of the samples relative to the depleted mantle range from 0.52 to 0.88 Ga. Nd model ages of the Borçka volcanic rocks are young (Table 2), suggesting a young lithospheric mantle source. The Borçka volcanic rocks are placed on the mantle array in between the depleted and the enriched quadrants. These values nearly correspond to those estimated for bulk earth, so are similar to those of other volcanics of the early Eocene age and the middle Eocene high-K granitoids from the Eastern Pontides (Karsli et al., 2007; Kaygusuz et al., 2011; Temizel et al., 2012; Topuz et al., 2005).

5. Discussion

5.1. Petrogenetic consideration

The geochemical fingerprints of the Borçka volcanic rocks are typical of subduction zone volcanic rocks (Baier et al., 2008; Elburg et al., 2002; Pearce, 1983; Thompson et al., 1984). The most basic samples of Borçka volcanics lack primitive rocks with Mg# > 70 or high compatible element abundances—for example, Ni > 200 ppm, Cr > 400 ppm—that are considered to represent magmas derived directly from the peridotitic mantle (Tatsumi and Eggins, 1995). The geochemical Sr and Nd isotopic compositions of the Borçka volcanic rocks in the Eastern Pontides, NE Turkey, provide constraints on the nature of the mantle source, the evolution processes of the parental magma, and the geodynamic setting. The principal evidences for such a generation are clearly illustrated below.

5.2. Magma evolution: fractional crystallization versus assimilation processes

The Borçka volcanic rocks have low Ni, Co, and MgO contents suggesting that the most mafic samples of the volcanics are not a product of primary magma. Harker variation diagrams show chemical trends consistent with fractional crystallization (Fig. 7). The lack

Civanköy Suite														
A33A	A44	A64	A71	A17B	A26	A32	A45a	A61	A67	A67A	A67B	A70	A74	A79
56.15	61.81	62.90	58.08	46.17	49.13	49.51	46.67	43.31	47.17	47.73	47.32	50.64	53.93	53.41
0.53	0.42	0.44	0.57	0.76	0.63	0.72	0.74	0.72	0.64	0.76	0.6	0.67	0.64	0.59
17.41	16.07	17.12	16.40	17.47	19.99	21.07	16.72	18.11	20.84	19.78	20.35	17.46	17.97	18.35
7.96	5.84	5.04	5.12	10.94	8.12	7.60	10.87	10.25	9.10	8.56	8.27	8.11	8.03	8.23
0.11	0.07	0.10	0.09	0.22	0.11	0.14	0.18	0.18	0.09	0.10	0.09	0.15	0.21	0.16
3.44	1.51	1.78	2.67	6.88	4.23	3.17	5.22	5.65	4.69	2.8	3.95	4.42	2.96	4.78
6.62	3.32	5.83	5.33	6.74	9.78	10.15	10.96	8.36	10.55	11.89	9.92	7.86	6.75	6.61
3.3	5.81	3.41	3.54	4.45	2.12	3.83	1.75	2.99	2.03	3.96	2.24	4.57	3.65	3.33
0.37	1.12	1.76	2.06	0.09	0.21	0.45	0.72	0.19	0.18	0.18	0.3	1.98	0.62	0.27
0.13	0.12	0.19	0.31	0.23	0.05	0.11	0.15	0.18	0.02	0.13	0.04	0.42	0.15	0.13
3.8	3.8	1.3	5.6	5.7	5.4	3.1	5.8	9.8	4.5	3.9	6.7	3.4	4.9	3.9
99.81	99.89	99.84	99.74	99.7	99.82	99.81	99.79	99.75	99.83	99.82	99.81	99.65	99.82	99.77
9.3	12.6	2.8	11.3	24.6	6.9	5.2	8.3	9.3	3.6	5.4	3.5	2.7	0.3	4.4
21	14	9	11	35	21	24	36	28	22	25	19	16	11	21
98	172	533	775	93	69	116	418	219	87	50	55	890	323	190
16.7	6.8	6.1	12.8	36.9	19.3	18.4	26.5	29.8	20.5	18	18.2	22	8.5	19.9
0.3	0.7	1.1	0.3	0.2	1.4	0.5	0.5	2.1	0.1	0.1	0.2	2.9	0.2	0.1
14.2	13.5	15.6	15	15.1	16.1	16.7	13.4	16.2	17.1	15.9	16.9	12	12.2	17.6
1.4	2.3	2.9	2.3	1.2	1.5	1.2	0.9	0.9	1.1	1.5	1	2.4	1.3	1.5
1.7	5.5	6.4	7.6	1.7	1.3	1.2	0.9	0.9	1	1.1	0.8	5.1	1.4	1.6
7.2	38.5	47.1	44.7	1	3.7	6.4	10	4.9	2.3	3	5	37.8	10.3	4.8
370.5	420.2	383.8	807.5	486.9	265.8	345.2	294.8	341.8	287	290.8	266.3	908.1	406.5	364.8
<0.1	0.4	0.3	0.5	0.1	<0.1	<0.1	0.1	0.1	<0.1	<0.1	<0.1	0.4	<0.1	<0.1
0.5	1.7	2.4	3.6	2.6	0.6	0.4	1.5	1	0.3	0.7	0.4	5.1	0.9	0.6
0.1	1.2	1.1	1	0.9	0.2	0.2	0.6	0.3	0.2	0.2	0.1	2	0.4	0.4
228	83	96	104	382	210	236	284	317	255	266	216	248	80	217
42.1	75.3	98	93.6	37.5	40.3	36.7	30.9	27.3	33.6	45.4	32.1	85.1	38.8	44.7
14.5	11.2	17.4	8.5	12.9	12.1	13.2	12.8	12.2	13.3	18.7	13	23.3	15.5	14
64.4	35.9	13.1	34.4	88.1	38.4	123.5	61.1	59.4	44.3	39.3	50.6	137.3	1.8	41.7
1.5	4.8	1.6	6.3	1.8	3.4	2.4	4.2	3.5	2.1	3.7	2	9.1	2.6	1.8
55	31	21	53	64	62	67	51	65	53	60	49	63	44	62
5.3	8.4	16.2	20.9	11.1	3.6	3.7	5.6	6.1	2.3	4.8	2.7	20.2	5.7	5.1
11.7	16	32.5	37.3	24.4	9	9.5	11.4	13.4	5.8	11.2	7.2	40.6	13.3	11.3
1.49	2.26	4.01	4.27	3.11	1.28	1.34	1.63	1.81	0.95	1.58	1.06	5.22	1.83	1.52
7.2	9.5	16.1	16.3	13.4	6.4	6	8.3	8.5	4.7	8.4	5.3	22.4	8.3	7
1.72	1.91	2.97	2.72	2.99	1.71	1.9	2.11	1.96	1.6	2.23	1.69	4.83	2.2	1.88
0.65	0.57	1.01	0.86	0.96	0.67	0.73	0.8	0.75	0.66	0.84	0.67	1.47	0.95	0.71
2.04	1.76	2.93	2.2	2.83	2.1	2.22	2.55	2.12	1.99	2.72	2.09	4.68	2.41	2.15
0.36	0.28	0.48	0.31	0.44	0.37	0.39	0.37	0.39	0.39	0.51	0.38	0.72	0.47	0.39
2.22	2.28	2.65	1.69	2.37	2.14	2.35	2.85	2.15	2.38	3.09	2.35	3.94	2.73	2.61
0.51	0.44	0.55	0.3	0.49	0.48	0.52	0.5	0.47	0.52	0.73	0.54	0.79	0.61	0.48
1.51	1.5	1.68	0.78	1.35	1.45	1.46	1.65	1.32	1.56	2.19	1.45	2.23	1.64	1.59
0.21	0.25	0.26	0.12	0.22	0.21	0.23	0.25	0.22	0.24	0.33	0.24	0.36	0.29	0.24
1.41	1.77	1.7	0.71	1.23	1.45	1.52	1.61	1.26	1.51	2.18	1.49	2.17	1.65	1.55
0.24	0.26	0.25	0.11	0.19	0.22	0.23	0.22	0.22	0.22	0.33	0.22	0.34	0.29	0.22
1.06	0.93	1.04	1.04	0.99	1.08	1.08	1.05	1.12	1.13	1.04	1.09	0.93	1.26	1.08
2.54	3.21	6.44	19.89	6.10	1.68	1.64	2.35	3.27	1.03	1.49	1.22	6.29	2.33	2.22
30	21	26	34	39	34	29	32	36	34	25	32	35	27	37

of negative Eu anomalies in the most primitive samples (Fig. 8) indicates that plagioclase was not a major fractionating mineral phase. Major and trace element compositions of the volcanic rocks indicate that clinopyroxene ± hornblende ± plagioclase ± magnetite ± apatite were important fractionating mineral phases in the petrogenesis of the rocks.

In calc-alkaline suites, Lambert and Holland (1974) used a CaO versus Y diagram to define J- and L-type trends, which lead to depletion and enrichment in Y relative to calc-alkaline series standard, respectively. In the Y versus CaO diagram (Fig. 10), nearly all the rocks plot on the Y depleted side of the standard calc-alkaline trend, defined as a J-type trend. This trend implies that pyroxene and hornblende played an important role in the evolution of the studied volcanics.

The variation in Ti, Zr, Y, and V within the suite of arc rocks is clearly related to the nature and proportion of crystallizing phases (Pearce and Norry, 1979). The SiO_2 versus Sr/Y diagram appears generally to be a result of plagioclase fractionation (Fig. 11). The crystallization of V, Fe–Ti oxides within volcanic rocks is reflected by a trend of decreasing Ti/Zr and V/Ti for residual melts (e.g., Nielsen et al., 1994; Pearce and Norry, 1979). Zr concentrations appear to be controlled almost exclusively by fractionation. Zr enrichment relative to Sm is often attributed to amphibole fractionation (Thirlwall et al., 1994). Besides, augite fractionation (Thirlwall et al., 1994) and magnetite fractionation (Tribuzio et al., 1999) may also exert an influence on the Zr/Sm ratio.

Many studies on arc magmatism confirm the importance of crustal assimilation, which leads to the modification of the trace elements and the isotopic composition of mantle-derived arc magmas (Thirlwall et al., 1996). Kaygusuz et al. (2011), Temizel and Arslan (2008, 2009), Temizel et al. (2012) argued for the contamination of the primary melt by mature and thickened arc crusts as an important feature of post-collisional Tertiary magmatism in the Eastern Pontides belt. However, Temizel and Arslan (2008) and Temizel et al. (2012) indicated that the assimilation and fractional crystallization (AFC) process played a significant role in the evolution of volcanic rocks in Ulubey (Ordu)

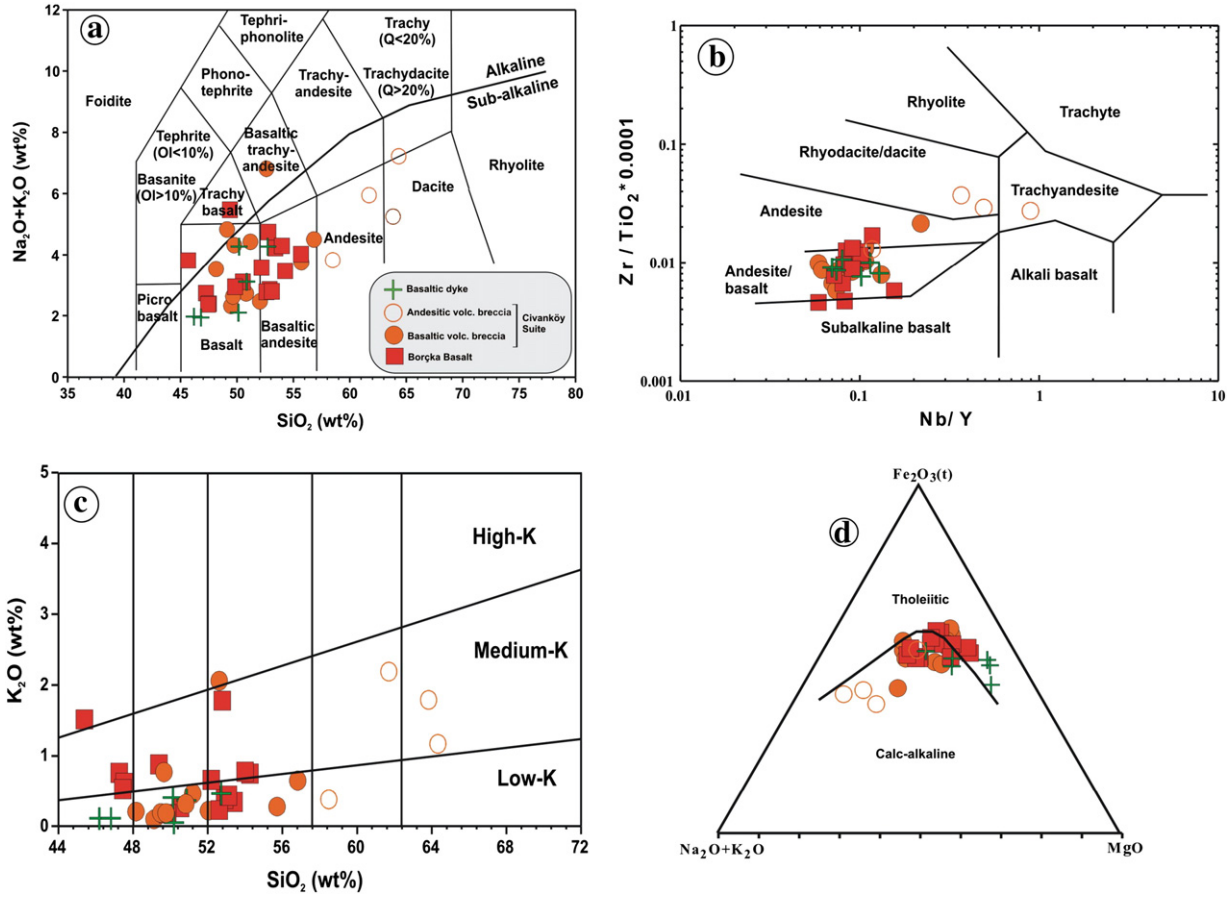

Fig. 6. Distributions of the investigated volcanic rocks on various geochemical classification diagrams. (a) $Na_2O + K_2O$ (wt.%) vs. SiO_2 (wt.%) diagram (Le Bas et al., 1986), (b) Zr/TiO_2*0.0001 vs. Nb/Y diagram (Winchester and Floyd, 1977), (c) SiO_2 (wt.%) vs. K_2O (wt.%) diagram (Le Maitre, 2002), (d) AFM ternary plot of the Borçka volcanics (alkaline–subalkaline dividing line and tholeiitic–calcalkaline dividing curve are from Irvine and Baragar, 1971).

area. The composition of these rocks was mainly modified by fractional crystallization rather than by AFC. In Fig. 12, the $(^{87}Sr/^{86}Sr)_i$ and $(^{143}Nd/^{144}Nd)_i$ ratios are plotted against SiO_2, MgO, Th, Sr, and Rb/Sr to evaluate the role of fractional crystallization (FC) or the AFC processes. Positive or negative trends attest to the fact that the magmas were affected by AFC processes, while nearly constant trends indicate significant crystallization.

The role of FC in the chemical evolution of the volcanics is evaluated using the least-squares method for the major elements. The compositions of clinopyroxene, hornblende, plagioclase, and magnetite of the rocks from the Borçka volcanics are used in the model. The calculations were performed based on the average composition of basaltic dyke and Borçka basalt as the parent, and Borçka basalt and Civanköy suite as the daughter from the volcanics. The results of the calculations are given in Table 3. The models for each groups mostly yield low residuals ($r^2 < 0.5$), suggesting that fractional crystallization is the main process with a minor assimilation for magmatic evolution of the Borçka volcanic rocks.

5.3. Source characteristics

The Borçka volcanic rocks are characterized by enrichments in LILE and LREE, and negative Nb, Ta, and Ti anomalies are features of subduction-related magmas and are commonly attributed to a mantle wedge source that was modified by metasomatic fluids derived from subducted slab or sediments (Cameron et al., 2003; Hawkesworth et al., 1991; Münker et al., 2004; Ringwood, 1990).

On the basis of $^{87}Sr/^{86}Sr$ versus Sr/Th relationships in a number of arcs, Hawkesworth et al. (1997) noted that high Sr/Th ratios are developed in rocks with low $^{87}Sr/^{86}Sr$ (~0.704). The rationale for using this plot is that as a result of the preferential mobilization of the LILE into hydrous fluids, high Sr/Th ratios will be a signature of the fluid phase. Sr isotope ratios might be expected to be variable, depending on whether the fluids have interacted mainly with altered basaltic crust (≥0.7047; Bickle and Teagle, 1992; Staudigel et al., 1995) or subducted sediment (>0.709). This indicates that the fluid components had similarly low $^{87}Sr/^{86}Sr$. Rocks from depleted and enriched arcs show (Fig. 13) a hyperbola that implies that high Sr/Th (and thus, LILE/HFSE) ratios are better developed in the more depleted arc rocks, whereas low Sr/Th is accompanied by high $^{87}Sr/^{86}Sr$. The Borçka volcanic rocks span an array (Sr/Th > 200; $^{87}Sr/^{86}Sr < 0.705$) similar to that of depleted arcs, and comply with a considerable fluid input to their sources.

The Borçka volcanics represent somewhat high and flat HREE patterns (Fig 8), indicating that the protolith may be garnet rich and garnet-rich residue after melt extraction. Instead, the patterns are consistent with the property of spinel in the mantle source. The source enrichment features in the Borçka volcanic rocks may be examined in the Th/Yb versus Ta/Yb (Pearce et al., 1990, Fig. 14) diagram. In this diagram, the Borçka volcanic rocks form a trend sub-parallel to the mantle array, but shifted to higher Th/Yb ratios. This suggests a melt derivation from a source, which had been

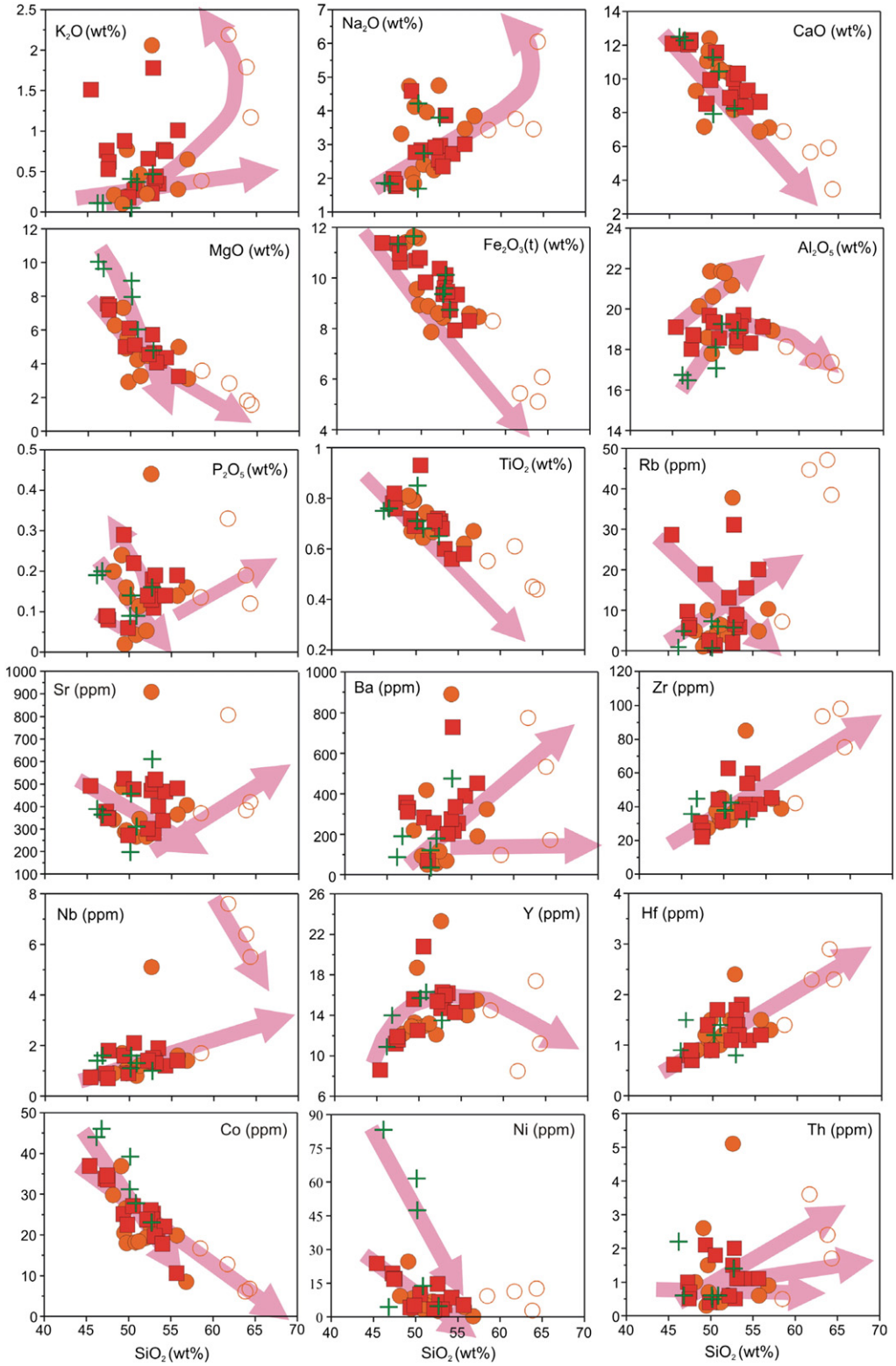

Fig. 7. SiO_2 (wt.%) vs. major oxides (wt.%) and trace element (ppm) variation diagrams for samples from the Borçka volcanic rocks (symbols are as in Fig. 6a).

previously enriched (or metasomatized) by fluids derived from earlier (i.e., pre-Eocene) subduction processes (e.g., Arslan et al., 2007; Kaygusuz et al., 2011; Temizel and Arslan, 2008; Temizel et al., 2012). Bradshaw and Smith (1994) and Smith et al. (1999) implied that since HFSE (such as Nb and Ta) are depleted in the lithospheric mantle relative to the LREE, high Nb/La ratios (~>1) indicate an OIB-like asthenospheric mantle source for basaltic magmas, and lower ratios (~<0.5) indicate a lithospheric mantle source. The Nb/La (0.15–0.21) and La/Yb (3–30) ratios of the most basic samples in the Borçka area suggest a lithospheric mantle source.

Borçka volcanic rocks, similar to arc volcanic, have higher La/Nb (2–7) and Ba/Nb (22–486) ratios compared to MORB, OIB, and intraplate basalts (Sun and McDonough, 1989; Fig. 15a). In the Ce/Pb versus Ce diagram (Fig. 15b), all the samples plot in the arc volcanic subfield.

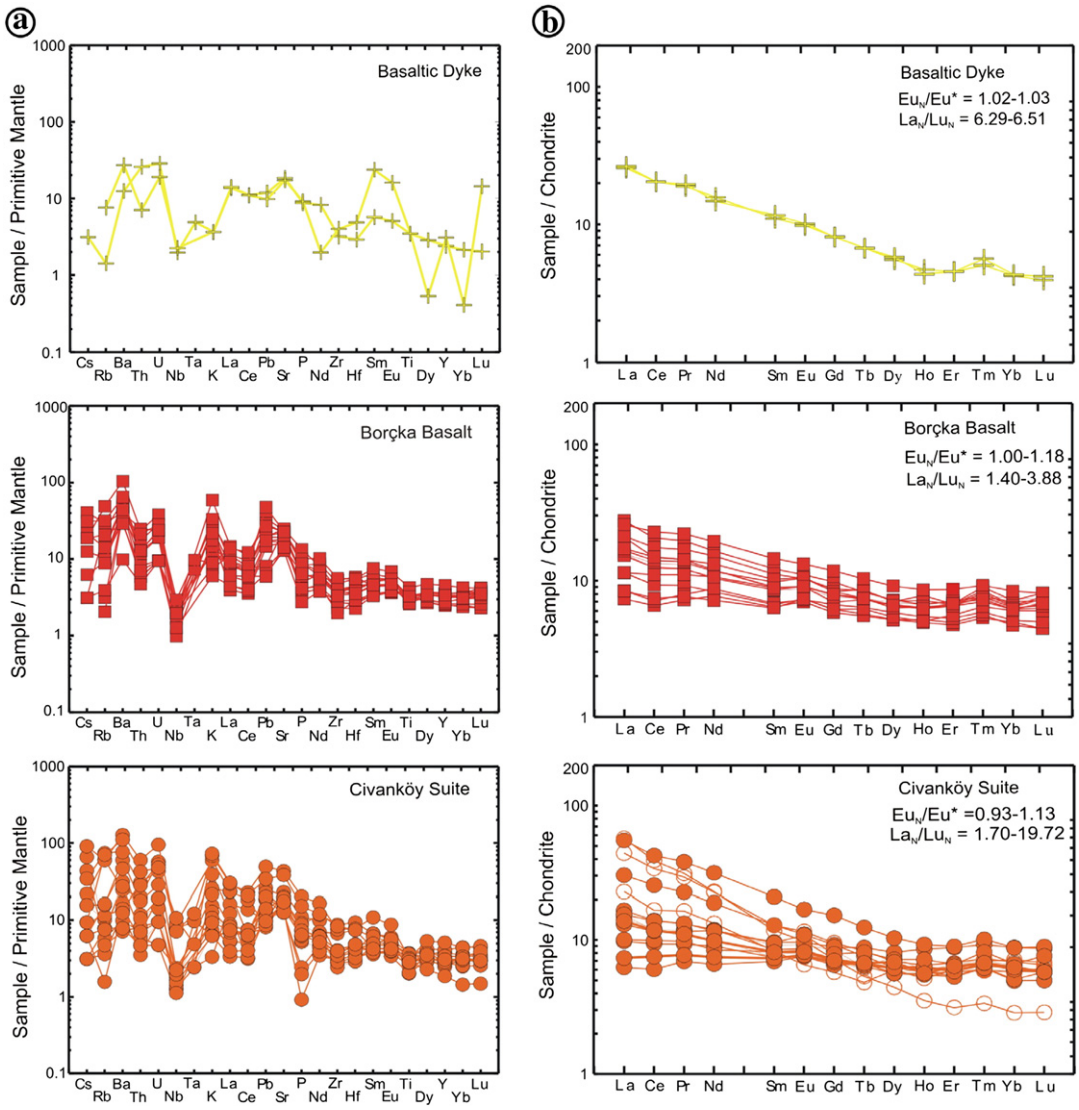

Fig. 8. (a) Primitive mantle-normalized (Sun and McDonough, 1989) multi-element spider diagrams and (b) chondrite-normalized (Boynton, 1984) rare earth element pattern plots for the Borçka volcanic rocks.

The average low Ce/Pb ratios (~8) of the most primitive samples differ considerably from those of oceanic basalts (~25; Gribble et al., 1998; Hofmann, 1988), suggesting that these rocks are not derived from normal asthenospheric mantle.

Sr and Nd isotope ratios of the Borçka volcanic rocks define a narrow field between bulk earth composition and depleted mantle (Fig. 9). Isotope ratios are very close to those of Eastern Pontides calc-alkaline volcanics (Kaygusuz et al., 2011; Temizel et al., 2012). Moreover, similar $^{87}Sr/^{86}Sr$ and $^{143}Nd/^{144}Nd$ isotope compositions support the genetic link between the mafic and more felsic rocks of the Borçka volcanic via fractional crystallization (Fig. 9).

On the basis of the combined trace element and the Sr–Nd isotope data, we concluded that the parental magma of the Borçka volcanic rocks was derived from partial melting of an enriched lithospheric mantle, which had been previously metasomatized by fluids derived from earlier subduction processes.

5.4. Geodynamic scenario for the Borçka volcanics

The Eastern Pontides was affected by a complex tectonic regime since late Paleocene–early Eocene (Okay and Şahintürk, 1997), and constitutes an upper Mesozoic–early Tertiary east–west-trending magmatic belt (Fig 1a). This belt is interpreted as an island arc developed in response to the northward subduction of the northern branch of Neotethys, resulting in the convergence of the Pontides in the north and the Tauride–Anatolide platform in the south (Okay and Şahintürk, 1997; Yılmaz et al., 1997). The closure of the Neo-Tethyan Ocean caused be a collision between the Pontides arc and the Tauride–Anatolide platform (Fig. 16a, b). Both the onset of subduction and the timing of the collision between the Pontides and the Tauride–Anatolide platform are a matter of debate (Akın, 1979; Boztuğ et al., 2004; Karsli et al., 2011; Robinson et al., 1995Tokel, 1977; Topuz et al., 2011). During the Paleocene–early Eocene time, the Eastern Pontides was above sea-level (Okay and Şahintürk, 1997), but based on structural data and the composition and timing of igneous activity, some authors (Boztuğ et al., 2006, 2007; Karsli et al., 2011; Okay and Şahintürk, 1997; Şengör and Yılmaz, 1981; Topuz et al., 2005, 2011; Yılmaz et al., 1997) propose a Paleocene–early Eocene (ca. 55 Ma) collision, resulting in crustal thickening and the regional uplift of the Eastern Pontides. Robinson et al. (1995) and Tokel (1977) considered that the middle Eocene volcanic rocks formed during the northward subduction of the Eastern Pontides and the subsequent collision occurred in the Oligocene (ca. 30 Ma).

Table 2
Sr and Nd isotope data for the Borçka volcanic rocks.

Sample	Rb (ppm)	Sr (ppm)	$^{87}Rb/^{86}Sr$	$^{87}Sr/^{86}Sr$	2σm	$(^{87}Sr/^{86}Sr)i$	Sm (ppm)	Nd (ppm)	$^{147}Sm/^{144}Nd$	$^{143}Nd/^{144}Nd$	$(^{143}Nd/^{144}Nd)i$	2σm	$\varepsilon_{Nd}(0)$	$\varepsilon_{Nd}(T)$ 46 Ma	T_{DM} (Ga)
A2	6.6	282	0.0678	0.704349	6	0.70430	2.03	8.50	0.1444	0.512866	0.512823	7	4.4	4.7	0.63
A5	2.0	471	0.0123	0.704423	7	0.70441	2.08	8.50	0.1479	0.512864	0.512819	4	4.4	4.7	0.66
A16	9.7	379	0.0742	0.704425	7	0.70438	1.54	5.90	0.1578	0.512901	0.512854	5	5.1	5.4	0.68
A25	6.3	350	0.0522	0.704415	6	0.70438	1.48	5.50	0.1627	0.512856	0.512807	5	4.3	4.4	0.88
A24	15.5	467	0.0963	0.704401	6	0.70434	1.98	7.40	0.1618	0.512879	0.512830	8	4.7	4.9	0.80
A73	1.3	477	0.0079	0.704233	7	0.70423	3.36	13.80	0.1472	0.512882	0.512838	9	4.8	5.0	0.61
A111	20.1	481	0.1212	0.704442	6	0.70436	2.37	9.40	0.1524	0.512878	0.512832	10	4.7	4.9	0.68
Basaltic dyke (46 Ma)															
A17A	0.9	389	0.0067	0.704409	5	0.70440	2.54	11.20	0.1371	0.512781	0.512780	5	3.6	3.9	0.66
Basaltic volcanic breccia (46 Ma)															
A70	37.8	908	0.1207	0.704401	6	0.70432	4.83	22.40	0.1304	0.512844	0.512805	8	4.0	4.4	0.56
Andesitic volcanic breccia (39.9 Ma)															
A64	47.1	384	0.3559	0.705148	5	0.70495	2.97	16.10	0.1150	0.512663	0.512633	7	0.5	0.9	0.75
A71	44.7	808	0.1605	0.704365	6	0.70427	2.72	16.30	0.1009	0.512766	0.512740	6	2.5	3.0	0.52

Note: $\varepsilon_{Nd} = ((^{143}Nd/^{144}Nd)_s/(^{143}Nd/^{144}Nd)_{CHUR} - 1) \times 10{,}000$, $(^{143}Nd/^{144}Nd)_{CHUR} = 0.512638$, and $(^{147}Sm/^{144}Sm)_{CHUR} = 0.1967$ (Jacobsen and Wasserburg, 1980). Nd model ages (TDM) are calculated with a depleted-mantle reservoir and present-day values of $^{143}Nd/^{144}Nd = 0.513151$ and $^{147}Sm/^{144}Sm = 0.219$ (Liew and Hofmann, 1988). The model ages were calculated using a linear isotopic ratio growth equation: $TDM = 1/\Lambda \times \ln(1 + ((^{143}Nd/^{144}Nd)_s - 0.51315) / ((^{147}Sm/^{144}Nd)_s - 0.2137))$.

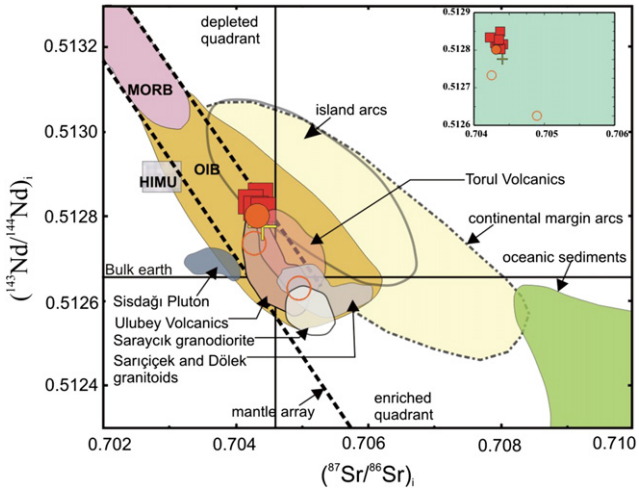

Fig. 9. Variation of initial $^{87}Sr/^{86}Sr$ vs. initial $^{143}Nd/^{144}Nd$ values. Sr–Nd isotopic compositions of the Eocene igneous and volcanic rocks from the Eastern Pontides. Data from Karsli et al. (2007, 2012a), Kaygusuz et al. (2011), Temizel et al. (2012), and Topuz et al. (2005). Compositions of MORB (Mid Ocean Ridge Basalt) and Mantle Array from Gill (1981), McCulloch et al. (1994) and Wilson (1989); HIMU (high μυ: mantle with high U/Th ratio) (symbols are as in Fig. 6a).

There is significant consensus about the Eocene magmatism in the Pontides formed during a post-collisional, extensional geodynamic setting (Arslan et al., 2009; Arslan et al., 2013; Aydin et al., 2008; Boztuğ and Harlavan, 2008; Boztuğ et al., 2004; Karsli et al., 2007, 2012a; Kaygusuz et al., 2011; Temizel et al., 2012; Topuz et al., 2005, 2011; Yılmaz and Boztuğ, 1996). Characteristics of isotopic and the whole rock geochemistry of the Borçka volcanic rocks indicate that the parental magma were derived from a partial melting of the lithospheric mantle, which had been previously metasomatized by fluids derived from an earlier subduction process. The partial melting of the lithospheric mantle could be due to two different reasons. These are

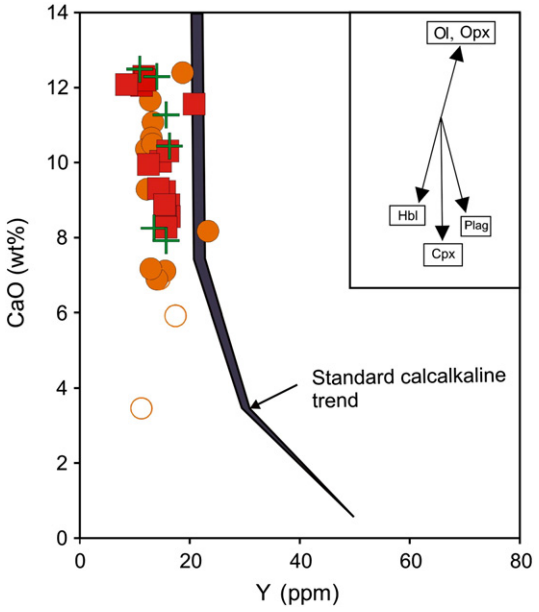

Fig. 10. CaO (wt.%) vs. Y (ppm) plot for the Borçka volcanic rocks. Shaded area represents the "standard" calcalkaline trend of Lambert and Holland (1974). The vectors show qualitative trends of the effect of fractional crystallization of common silicates (symbols are as in Fig. 6a).

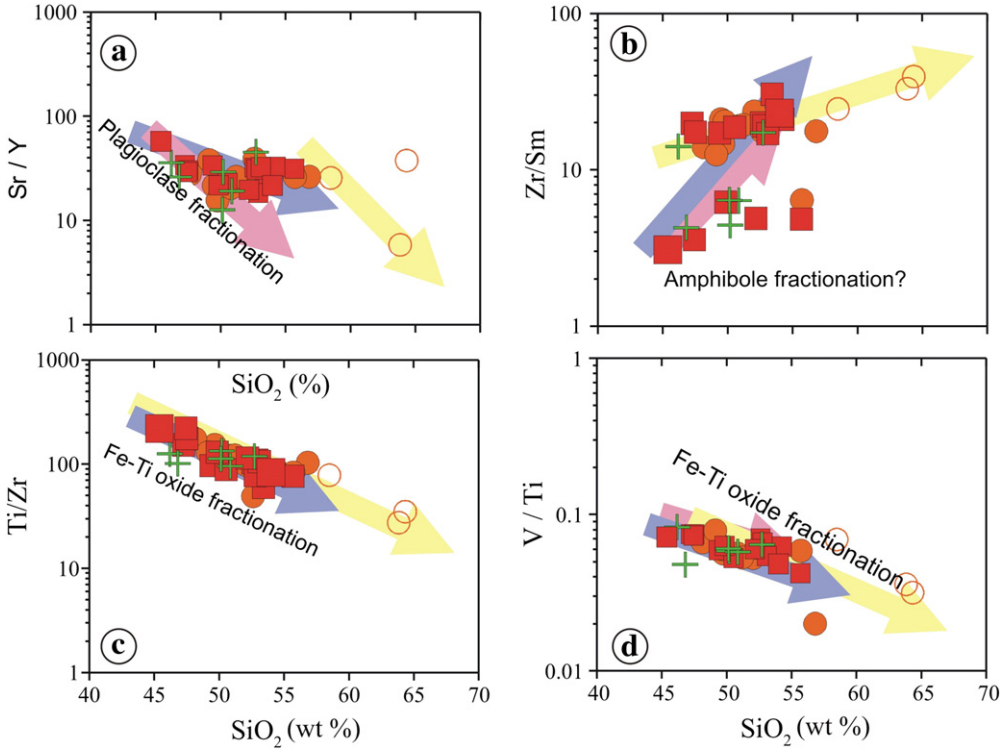

Fig. 11. Whole rock trace-element ratios plotted vs. silica for volcanic rocks from the Borçka area. (a) Sr/Y reflects plagioclase fractionation within volcanics, (b) variation in Zr/Sm is often attributed primarily to amphibole fractionation. However, clinopyroxene and magnetite fractionation may also exert an influence on this ratio, (c,d) Ti/Zr and V/Ti variation show a strong signature of Fe–Ti oxide fractionation, but also may have been affected by amphibole fractionation (symbols are as in Fig. 6a).

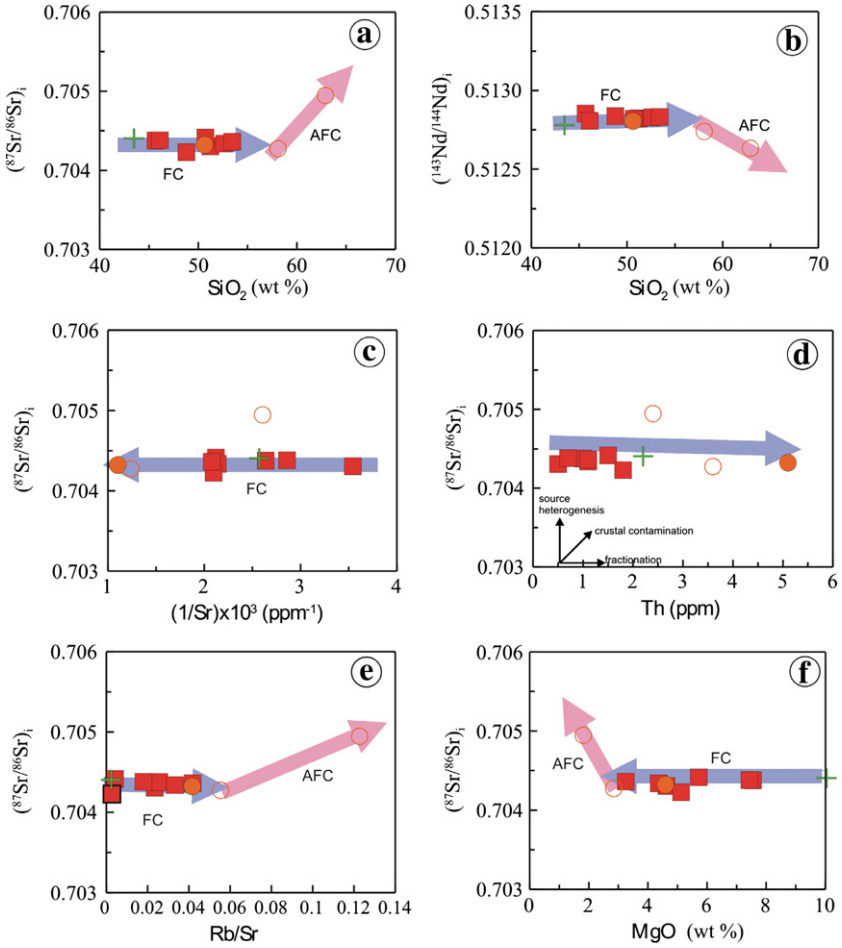

Fig. 12. Variation diagrams of $(^{87}Sr/^{86}Sr)_i$ and $(^{143}Nd/^{144}Nd)_i$ vs. SiO_2 (wt.%), $(1/Sr) \times 10^3$ (ppm^{-1}), Th (ppm), Rb/Sr and MgO (wt.%) from the Borçka volcanic rocks (symbols are as in Fig. 6a)

Table 3
Major element oxide fractional crystallization modeling for Borçka volcanic rocks.

		Stage 1: Basaltic dyke–Borçka basalt		
		Parent	Daughter	Calculated
		Average (n = 2)	Observed (n = 16)	
SiO_2		43.70	49.71	50.71
TiO_2		0.71	0.68	0.96
Al_2O_3		15.60	18.41	18.18
FeOt		10.81	9.48	9.61
MnO		0.19	0.19	0.30
MgO		9.25	4.96	6.18
CaO		11.64	9.57	9.52
Na_2O		1.74	2.71	3.80
K_2O		0.10	0.62	0.20
P_2O_5		0.19	0.14	0.53
Fractionating minerals, wt.%	Plagioclase (n = 15)			26.60
	Clinopyroxene (n = 20)			18.38
	Olivine (n = 5)			11.65
	Hornblende (n = 25)			
	Magnetite (n = 35)			4.53
Residual melt, wt.%				32.83
Sum residuals squared	(r^2)			0.30
		Stage 2: Borçka basalt–Civanköy suite		
		Parent	Daughter	Calculated
		Average (n = 16)	Observed (n = 15)	
SiO_2		49.71		52.01
TiO_2		0.68		0.71
Al_2O_3		18.41		18.38
FeOt		9.48		8.14
MnO		0.19		0.11
MgO		4.96		4.02
CaO		9.57		8.28
Na_2O		2.71		3.47
K_2O		0.62		0.80
P_2O_5		0.14		0.18
Fractionating minerals, wt.%	Plagioclase (n = 15)			23.53
	Clinopyroxene (n = 20)			13.26
	Olivine (n = 5)			
	Hornblende (n = 25)			32.46
	Magnetite (n = 35)			4.65
Residual melt, wt.%				25.90
Sum residuals squared	(r^2)			0.18

Total Fe as FeO^{tot}.
Mineral compositions used for each step of modeling are an average value of mineral compositions given in Supplementary Table 1. The composition of the mineral chemistry of olivine is taken from Koçevyan Basalt in Temizel and Arslan (2005, 2008).

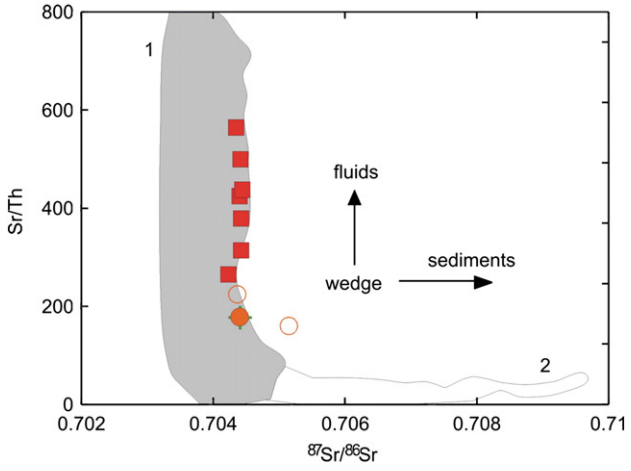

Fig. 13. $^{87}Sr/^{86}Sr$ vs. Sr/Th variations in Borçka volcanic rocks. Fields 1 and 2 enclose data from arcs considered incompatible element depleted and enriched, respectively, by Hawkesworth et al. (1997). The arrows show the sense of enrichment predicted from addition of fluid and sedimentary components to the mantle wedge (symbols are as in Fig. 6a).

(1) due to the adiabatic decompression resulting from a lithospheric extension of uplift, and (2) because of an increase in heat from the upwelling asthenospheric mantle. In the region, middle-late Eocene magmatism was considered to have formed by a combination of both mechanisms. The required heat flux for partial melting may have been supplied by the upwelling of the asthenosphere.

A similar model was advocated by Pearce et al. (1990) for Eastern Anatolia, Aldanmaz et al. (2000) and Altunkaynak and Dilek (2006) for Western Anatolia, İlbeyli et al. (2004) and Keskin et al. (2008) for central Anatolia, and Aslan (2010), Karsli et al. (2011a, 2012), Kaygusuz et al. (2011), and Temizel et al. (2012) for the Eastern Pontides. Slab break-off (Davies and von Blanckenburg, 1995), lithosphere delamination (Bird, 1979; Kay and Kay, 1993), and convective removal of the lithosphere (Houseman et al., 1981) are the main mechanisms proposed to explain the magmatism in post-collisional and post-orogenic settings. In case of the Borçka volcanic rocks, a generation from an enriched lithospheric mantle is documented by major and trace element features, Sr–Nd isotope characteristics, weak negative Eu anomalies, positive ε_{Nd} (t) values, homogenous and low initial $^{87}Sr/^{86}Sr$ values (~0.704) of the samples. Karsli et al. (2010b, 2011) and Topuz et al. (2011) proposed that the first stage of the post-collision extensional

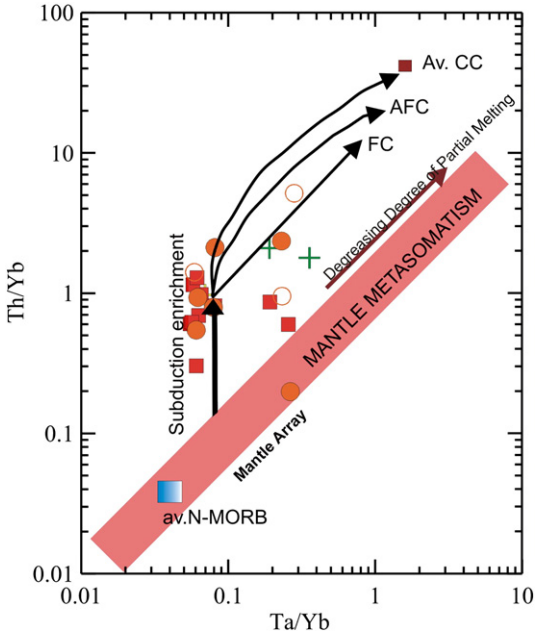

Fig. 14. Th/Yb vs. Ta/Yb diagram (after Pearce et al., 1990) for the Borçka volcanics. The inset diagram shows the variations of Th/Tb with changing silica contents of the rocks. Average N-MORB composition and average CC (Continental Crust) are from Sun and McDonough (1989) and Taylor and McLennan (1985), respectively. Vectors showing inferred effects of fractional crystallization (FC), assimilation-fractional crystallization (AFC), subduction enrichment and mantle metasomatism are from Pearce et al. (1990) (symbols are as in Fig. 6a).

event that followed the crustal thickening began at 50 Ma. At 46–40 Ma, slab break-off cannot be suggested as a dynamic model for the generation of the Eocene magmatism, because the phase, which is responsible for adakite-like melt generation, formed in the Eastern Pontides (Karsli et al., 2011; Topuz et al., 2011). Aydin et al. (2008), Karsli et al. (2012a) and Temizel et al. (2012) suggested that Tertiary volcanism is closely related to lithospheric thinning induced by local faulting. The upwelling of hot asthenospheric material results in thermal perturbation, and this thermal activity causes the initial melting of the lithospheric mantle, metasomatized by the earlier subduction event. This process requires an extensional regime of a short period in the compression orogenic belt (Arslan and Aslan, 2006; Arslan et al., 2013; Karsli et al., 2012a; Kaygusuz et al., 2011; Okay and Şahintürk, 1997; Temizel et al., 2012). As seen in Fig. 16a, b and c, following the northward subduction of the Neo-Tethyan Ocean through the late Cretaceous, the collision between the Pontides and Anatolide–Toride platform in the Paleocene and then slab break-off of the Neotethyan oceanic slab was an inevitable geodynamic event that occurred before the middle Eocene. Extensional regime in this region can be explained by post-collisional crustal thinning (Fig. 16d) (Topuz et al., 2005) (Fig. 16e, f) and delamination of the thickened crust (Arslan et al., 2013; Karsli et al., 2010b, 2012a; Temizel et al., 2012). All these events, causing the loss of pressure over the asthenosphere, should have accelerated the asthenospheric uplift in the middle Eocene. This asthenospheric upwelling caused partial melting of chemical enriched subcontinental lithospheric mantle in an extensional setting in the Eastern Pontides throughout middle Eocene time (Fig. 16g).

6. Conclusions

1. The middle Eocene Borçka volcanic rocks are composed of Borçka basalt (basaltic lava and pillow lava), Civanköy suite (basaltic–andesitic breccia and tuff), and basaltic dykes. They show porphyric, microlitic–porphyric, hyalo-microlitic porphyric, hyalopilitic, poikilitic, glomeroporphyric, and rarely intersertal, intergranular, and fluidal textures.
2. The ^{40}Ar–^{39}Ar dating of the hornblende separates from various lava flows yielded the ages of 46.0 ± 0.8 to 39.9 ± 0.5 Ma.
3. The volcanic rocks display tholeiitic to calc-alkaline character, with low and medium-K contents. All samples from the Borçka volcanic series display similar geochemical features, which are characterized by the enrichment of LILE and LREE and depletion of HFSE without Eu anomalies, suggesting similar parental magma and petrogenetic scenario.
4. Fractional crystallization (FC) with minor contamination by upper crustal materials, occurred during the evolution of the volcanic rocks with pyroxene, hornblende, plagioclase, and Fe–Ti oxides being the most important fractionating mineral phases.
5. The Borçka volcanic rocks have initial $^{87}Sr/^{86}Sr$ values varying between 0.70423 and 0.70495, and initial $^{143}Nd/^{144}Nd$ values between 0.51263 and 0.51285. These isotopic features, in conjunction with their geochemical characters, suggest that the parental magma of Borçka volcanic rocks originated from melting of a young lithospheric

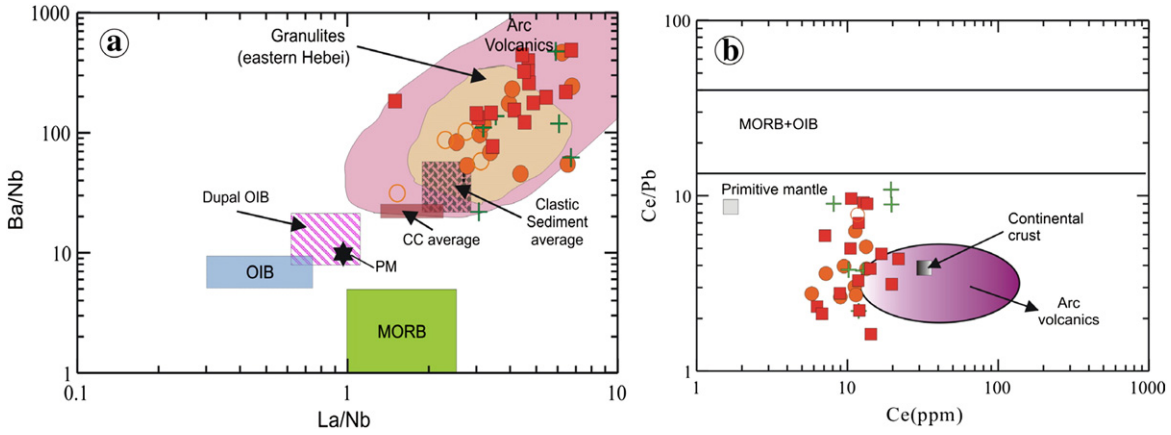

Fig. 15. (a) Ba/Nb vs. La/Nb (Jahn et al., 1999), (b) Ce/Pb vs. Ce (ppm) plots of the Borçka volcanic rocks. Data sources for reference: Arc volcanics and Archean granulites from eastern Hebei (data from Jahn and Zhang, 1984); PM (Primitive mantle; Sun and McDonough, 1989); CC average (Continental Crust average; Taylor and McLennan, 1985; Condie, 1993), Clastic Sediment average (Condie, 1993); MORB (Mid-Ocean Ridge Basalts), OIB (Ocean-island Basalt) and Dupal-OIB (Le Roex, 1987) in (a) and Primitive Mantle (Hofmann, 1988); Continental Crust, MORB, OIB and Arc Volcanics (Schmidberger and Hegner, 1999) in (b) (symbols are as in Fig. 6a).

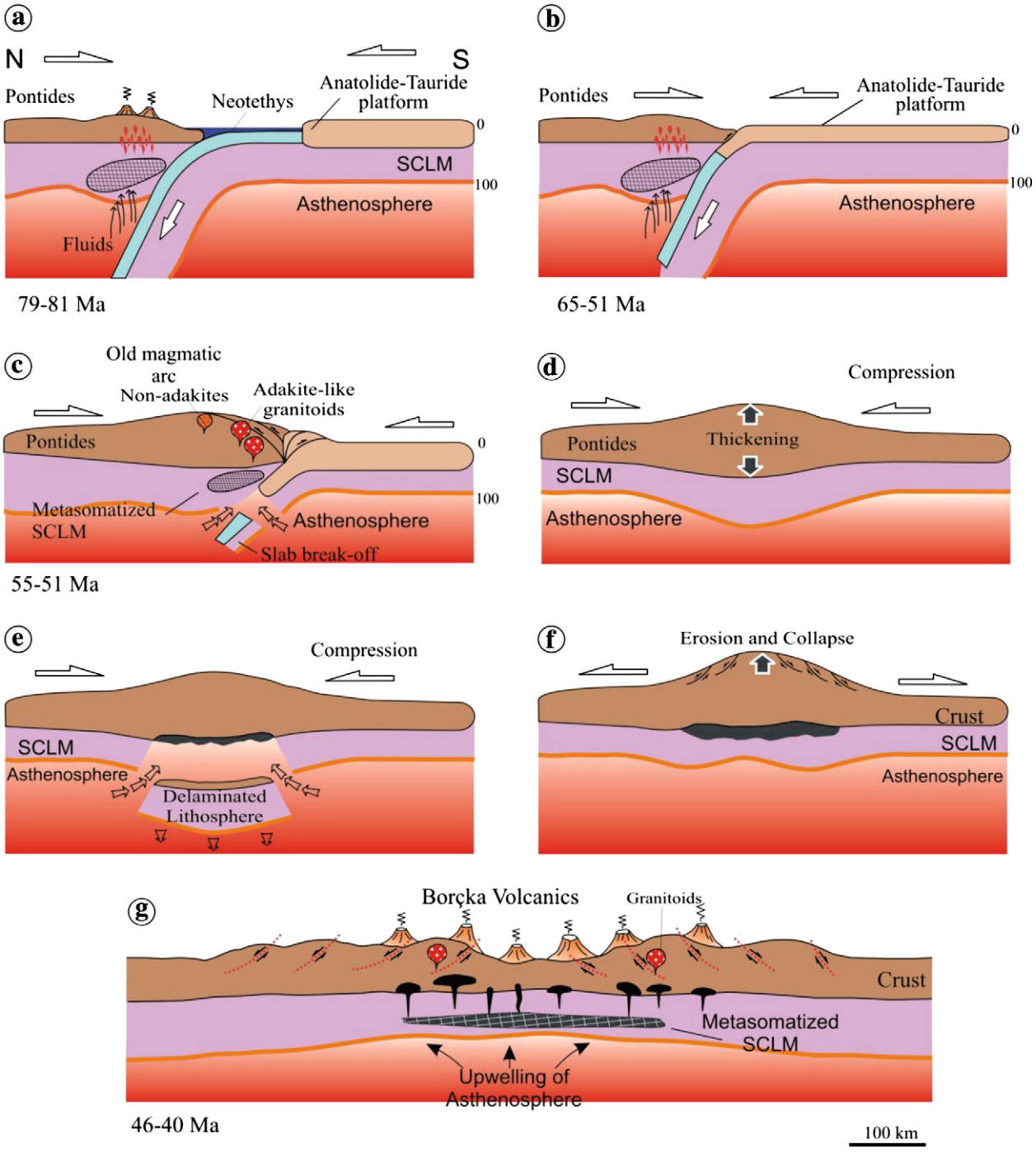

Fig. 16. Schematic diagram showing the tectonic evolution of the area studied between 81 and 40 Ma (a–g) and magmatic activity at ~46–40 Ma in Eastern Pontides, NE Turkey.

mantle, metasomatized by fluids derived from the subducted slab during the late Mesozoic time.

6. The Eocene volcanic rocks derived from subduction-induced enriched lithospheric mantle source should be related to the thinning of young lithosphere caused by extensional regime developed by lithospheric delamination geodynamics occurring in the Eastern Pontides.

Acknowledgments

This study is the PhD thesis of E. Aydınçakır and was financially supported by the Scientific Research Foundation of Karadeniz Technical University (Project #: 2008.112.005.5). We are most grateful to Bin Chen of the Isotopic Laboratory in the Institute of Geology, Chinese Academy of Geological Sciences in Beijing, for the isotopic analyses. Recommendations about the geodynamic evolution of the region from Abdurrahman Dokuz are gratefully acknowledged. We are also grateful to the editor in chief Nelson Eby, Şafak Altunkaynak and anonymous reviewer for critical and constructive comments to improve our paper. Wendy Kasap is gratefully acknowledged for her English editing. We thank Mürşid Öztürk and Hüseyin ASAN for their help in the field.

Appendix A. Supplementary data

Supplementary data to this article can be found online at http://dx.doi.org/10.1016/j.lithos.2013.04.007.

References

Adamia, S.A., Lordkipanidze, M.B., Zakariadze, G.S., 1977. Evolution of an active continental margin as exemplified by the Alpine history of the Caucasus. Tectonophysics 40, 183–199.

Akın, H., 1979. Geologie, Magmatismus und Lager-staettenbidung im ostpontischen Gebirge-Turkei aus der Sicht der Plattentektonik. Geologische Rundschau 68, 253–283.

Aldanmaz, E., Pearce, J.A., Thirlwall, M.F., Mitchell, J.G., 2000. Petrogenetic evolution of late Cenozoic, post-collision volcanism in western Anatolia, Turkey. Journal of Volcanology and Geothermal Research 102, 67–95.

Altunkaynak, S., 2007. Collision-driven slab breakoff magmatism in Northwestern Anatolia, Turkey. Journal of Geology 115, 63–82.

Altunkaynak, Ş., Dilek, Y., 2006. Timing and nature of postcollisional volcanism in western Anatolia and geodynamic implications. In: Dilek, Y., Pavlides, S. (Eds.), Postcollisional Tectonics and Magmatism in the Mediterranean Region and Asia: Geological Society of America, Special Paper, 409, pp. 321–351.

Arslan, M., Aliyazıcıoğlu, İ., 2001. Geochemical and petrological characteristics of the Kale (Gümüshane) volcanic rocks: implications for the Eocene evolution of eastern Pontide arc volcanism, northeast Turkey. International Geology Review 43, 595–610.

Arslan, M., Aslan, Z., 2006. Mineralogy, petrography and whole-rock geochemistry of the Tertiary granitic intrusions in the Eastern Pontides, NE Turkey. Journal of Asian Earth Sciences 27, 177–193.

Arslan, M., Tüysüz, N., Korkmaz, S., Kurt, H., 1997. Geochemistry and petrogenesis of the eastern Pontide volcanic rocks, northeast Turkey. Chemi der Erde 57, 157–187.

Arslan, M., Boztuğ, D., Temizel, İ., Kolayli, H., Şen, C., Abdioğlu, E., Ruffet, G., Harlavan, Y., 2007. $^{40}Ar/^{39}Ar$ geochronology and Sr–Pb isotopic evidence of post-collisional extensional volcanism of the Eastern Pontide paleo-arc, NE Turkey. Special Supplement, 17th Annu. V.M. Goldschmidt Conference, Geochronology of Tectonic Processes. Geochimica et Cosmochimica Acta 71 (15S), A38.

Arslan, M., Temizel, İ., Boztuğ, D., Abdioğlu, E., Kolayli, H., Yücel, C., 2009. Petrochemistry, $^{40}Ar/^{39}Ar$ geochronology and Sr–Pb isotope geochemistry of the Tertiary volcanics in Eastern Pontide southern zone, NE Turkey: geodynamic evolution related to slab break-off and transtensional tectonics. 2: International Symposium on the Geology of the Black Sea Region Abstract Book, p. 24.

Arslan, M., Temizel, İ., Abdioğlu, E., Kolaylı, H., Yücel, C., Boztuğ, D., Şen, C., 2013. $^{40}Ar–^{39}Ar$ dating, whole-rock and Sr–Nd–Pb isotopic geochemistry of post-collisional Eocene volcanic rocks in the southern part of the Eastern Pontides (NE Turkey): implications for magma evolution in extension-induced origin. Contribution to Mineralogy and Petrology. http://dx.doi.org/10.1007/s00410-013-0868-3.

Aslan, Z., 2010. U–Pb zircon SHRIMP age, geochemical and petrographical characteristics of tuffs within calc-alkaline Eocene volcanics around Gümüşhane (NE Turkey), Eastern Pontides. Neues Jahrbuch für Mineralogie 187 (3), 329–346.

Aydin, F., Karsli, O., Chen, B., 2008. Petrogenesis of the Neogene alkaline volcanics with implications for post collisional lithospheric thinning of the Eastern Pontides, NE Turkey. Lithos 104, 249–266.

Aydin, F., Thompson, R., Karsli, O., Uchida, H., Burt, J.B., Downs, R.T., 2009. C2/c pyroxene phenocrysts from there potassic series in Neogene alkaline volcanics, NE Turkey: their crystal chemistry with petrogenetic significance as a indicator of P–T conditions. Contributions to Mineralogy and Petrology 158, 131–147.

Aydınçakır, E., 2012. Petrography, Geochemistry and Petrogenesis of the Borçka (Artvin, NE Turkey) Area Tertiary Volcanics. PhD thesis Karadeniz Technical University, Trabzon (241 pp.).

Baier, J., Audetat, A., Kepler, H., 2008. The origin of the negative niobium tantalum anomaly in subduction zone magmas. Earth and Planetary Science Letters 267, 290–300.

Bazhenov, M.L., Burtman, V.S., 2002. Eocene palaeomagmatism of the Caucasus (southwest Georgia): oroclinal bending in the Arabian syntaxis. Tectonophysics 344, 247–259.

Bickle, M.J., Teagle, D.A.H., 1992. Strontium alteration in the Troodos ophiolite: implications for fluid fluxes and geochemical transport in mid-ocean ridge hydrothermal systems. Earth and Planetary Science Letters 113, 219–237.

Bird, P., 1979. Continental delamination and the Colorado Plateau. Journal of Geophysical Research 84, 7561–7571.

Boynton, W.V., 1984. Cosmochemistry of the rare earth elements: meteorite studies. In: Henderson, P. (Ed.), Rare Earth Element Geochemistry. Elsevier, Amsterdam, pp. 63–114.

Boztuğ, D., Harlavan, Y., 2008. K–Ar ages of granitoids unravel the stages of Neo-Tethyan convergence in the eastern Pontides and central Anatolia, Turkey. International Journal of Earth Sciences 97, 585–599.

Boztuğ, D., Jonckheere, R.C., Wagner, G.A., Yeğingil, Z., 2004. Slow Senonian and fast Paleocene–Early Eocene uplift of the granitoids in the Central Eastern Pontides, Turkey: apatite fission-track results. Tectonophysics 382, 213–228.

Boztuğ, D., Erçin, A.İ., Kuruçelik, M.K., Göç, D., Kömür, İ., İskenderoğlu, A., 2006. Geochemical characteristics of the composite Kaçkar batholith generated in a Neo-Tethyan convergence system, Eastern Pontides, Turkey. Journal of Asian Earth Sciences 27, 286–302.

Boztuğ, D., Jonckheere, R.C., Wagner, G.A., Erçin, A.I., Yeğingil, Z., 2007. Titanite and zircon fission-track dating resolves successive igneous episodes in the formation of the composite Kaçkar batholith in the Turkish eastern Pontides. International Journal of Earth Sciences 96, 875–886.

Bradshaw, T.K., Smith, E.I., 1994. Polygenetic Quaternary volcanism at Crater Flat, Nevada. Journal of Volcanology and Geothermal Research 63, 165–182.

Cameron, B.I., Walker, J.A., Carr, M.J., Patino, L.C., Matias, O., Feigenson, M.D., 2003. Flux versus decompression melting at stratovolcanos in southeastern Guatemala. Journal of Volcanology and Geothermal Research 119, 21–50.

Çamur, M.Z., Güven, T.B., Er, M., 1996. Geochemical characteristics of the eastern Pontide volcanics: an example of multiple volcanic cycles in arc evolution. Turkish Journal of Earth Sciences 5, 123–144.

Çapkınoğlu, Ş., 2003. First records of conodonts from the Permo-Carboniferous of Demirözü (Bayburt), Eastern Pontides, NE Turkey. Turkish Journal of Earth Sciences 12, 199–217.

Çoban, H., 1997. Olucak (Gumushane) ve dolayinin jeolojisi, petrografisi ve jeokimyasi. PhD thesis S.D.Ü. Fen Bilimleri Enstitüsü, p. 257 (unpublished).

Condie, K.C., 1993. Chemical composition and evolution of the upper continental crust: contrasting results from surface samples and shales. Chemical Geology 104, 1–37.

Davies, J.H., von Blanckenburg, F., 1995. Slab breakoff: a model of lithospheric detachment and its test in the magmatism and deformation of collisional orogens. Earth and Planetary Science Letters 129, 85–102.

Dilek, Y., Imamverdiyev, N., Altunkaynak, Ş., 2010. Geochemistry and tectonics of Cenozoic volcanism in the Lesser Caucasus (Azerbaijan) and the peri-Arabian region: collision-induced mantle dynamics and its magmatic fingerprint. International Geology Review 52, 536–578.

Dokuz, A., Tanyolu, E., 2006. Geochemical constraints on the provenance, mineral sorting and subaerial weathering of lower Jurassic and Upper Cretaceous clastic rocks from the Eastern Pontides, Yusufeli (Arvin), NE Turkey. Turkish Journal of Earth Sciences 15, 181–209.

Dokuz, A., Karsli, O., Chen, B., Uysal, I., 2010. Sources and petrogenesis of Jurassic granitoids in the Yusufeli area, Northeastern Turkey: implications for pre- and post-collisional lithospheric thinning of the Eastern Pontides. Tectonophysics 480, 259–279.

Dokuz, A., 2011. A slab detachment and delamination model for the generation of Carboniferous high-potassium I-type magmatism in the Eastern Pontides, NE Turkey: Köse composite pluton. Gondwana Research 19, 926–944.

Elburg, M.A., Bergen, M.V., Hoogewerff, J., Foden, J., Vroon, P., Zulkarmain, I., Nasution, A., 2002. Geochemical trends across an arc–continent collision zone: magma sources and slab-wedge transfer processes below the Pantar Strait volcanoes, Indonesia. Geochimica et Cosmochimica Acta 66, 2771–2789.

Gill, J.B., 1981. Orogenic Andesites and Plate Tectonics. Springer, Berlin 390 pp.

Gribble, R.F., Stern, R.J., Newman, S., 1998. Chemical and isotopic composition of lavas from the northern Mariana Trough: implications for magmagenesis in backarc basins. Journal of Petrology 39, 125–154.

Hall, C.-M., Farrell, J.W., 1995. Lazer $^{40}Ar/^{39}Ar$ ages of tephra from Indian Ocean deep-sea sediments: the points for the astronomical and geomagnetic polarity time scales. Earth and Planetary Science Letters 133, 327–338.

Hawkesworth, C.J., Hergt, J.M., McDermott, F. Ve, Ellam, R.M., 1991. Destructive margin magmatism and the contributions from the mantle wedge and subducted crust. Australian Journal of Earth Sciences 38, 577–594.

Hawkesworth, C.J., Turner, S., McDermott, F., Peate, D., van Calsteren, P., 1997. U–Th isotopes in arc magmas: implications for element transfer from the subducted crust. Science 276, 551–555.

Hofmann, A.W., 1988. Chemical differentiation of the Earth: the relationship between mantle, continental crust and oceanic crust. Earth and Planetary Science Letters 90, 297–314.

Houseman, G.A., McKenzie, D.P., Molnar, P., 1981. Convective instability of a thickened boundary layer and its relevance for the thermal evolution of the continental convergent belts. Journal of Geophysical Research 86, 6115–6132.

İlbeyli, N., Pearce, J.A., Thirlwall, M.F., Mitchell, J.G., 2004. Petrogenesis of collision related plutonic in Central Anatolia, Turkey. Lithos 72, 163–182.

Irvine, T.N., Baragar, W.R.A., 1971. A guide to the chemical classification of common volcanic rocks. Canadian Journal of Earth Sciences 8, 523–548.

Jahn, B.M., Zhang, Z.Q., 1984. Archean granulite gneisses from eastern Hebei Province, China: rare earth geochemistry and tectonic implications. Contributions to Mineralogy and Petrology 85, 224–243.

Jahn, B.M., Wu, F.Y., Lo, C.H., 1999. Crust–mantle interaction induced by deep subduction of the continental crust: geochemical and Sr–Nd isotopic evidence from post-collisional mafic–ultramafic intrusions of the northern Dabie Complex, Central China. Chemical Geology 157, 119–146.

Kandemir, R., 2004. Sedimentary Characteristics and Depositional Conditions of Lower–Middle Jurassic Şenköy Formation in and Around Gümüşhane. Unpublished PhD thesis Karadeniz Technical University, Trabzon, Turkey (274 pp.).

Kandemir, R., Lerosey-Aubril, R., 2011. First report a trilobite in the Carboniferous of Eastern Pontides, NE Turkey. Turkish Journal of Earth Sciences 20, 179–183.

Kandemir, R., Yılmaz, C., 2009. Lithostratigraphy, facies, and deposition environment of the lower Jurrassic Ammonitico Rosso type sediments (ARTS) in the Gümüşhane, area, NE Turkey: implications for the opening of the northern branch of the Neo-Tethys Ocean. Journal of Asian Earth Sciences 34, 586–598.

Karsli, O., Aydın, F., Sadıklar, B., 2004. The morphology and chemistry of K-feldsper megacrysts from İkizdere Pluton: evidence for acid and basic magma interactions in granitoid rocks, NE Turkey. Chemie der Erde-Geochemistry 64, 155–170.

Karsli, O., Chen, B., Aydın, F., Şen, C., 2007. Geochemical and Sr–Nd–Pb isotopic compositions of the Eocene Dölek and Sarıçiçek Plutons, Eastern Turkey: implications for magma interaction in the genesis of high-K calc-alkaline granitoids in a post-collision extensional setting. Lithos 98, 67–96.

Karsli, O., Dokuz, A., Uysal, İ., Aydın, F., Bin, C., Kandemir, R., Wijbrans, J.R., 2010a. Relative contributions of crust and mantle to generation of Campanian high-K calc-alkaline I-type granitoids in a subduction setting, with special reference to the Harşit pluton, Eastern Turkey. Contribution to Mineralogy and Petrology 160, 467–487.

Karsli, O., Dokuz, A., Uysal, İ., Aydın, F., Kandemir, R., Wijbrans, J.R., 2010b. Generation of the Early Cenozoic adakitic volcanism by partial melting of mafic lower crust, Eastern Turkey: implication for crustal thickening to delamination. Lithos 114, 109–120.

Karsli, O., Uysal, İ., Ketenci, M., Dokuz, A., Aydın, F., Chen, B., Kandemir, R., Wijbrans, J., 2011. Adakite-like granitoid porphyries in Eastern Pontides, NE Turkey: potential parental melts and geodynamic implications. Lithos 127, 354–372.
Karsli, O., Dokuz, A., Uysal, İ., Ketenci, M., Chen, B., Kandemir, R., 2012a. Deciphering the shoshonitic monzonites with I-type characteristics, the Sisdağı pluton, NE Turkey: magmatic response to continental lithospheric thinning. Journal of Asian Earth Sciences 51, 45–62.
Karsli, O., Caran, Ş., Dokuz, A., Çoban, H., Chen, Bin, Kandemir, R., 2012b. A-type granitoids from the Eastern Pontides, NE Turkey: records for generation of hybrid A-type rocks in a subduction-related environment. Tectonophysics 530–531, 208–224.
Kay, R.W., Kay, S.M., 1993. Delamination and delamination magmatism. Tectonophysics 219, 177–189.
Kaygusuz, A., Aydınçakır, E., 2009. Mineralogy, whole rock and Sr–Nd isotope geochemistry of mafic microgranular enclaves in Cretaceous Dağbaşı granitoids, eastern Pontides, NE Turkey: evidence of magma mixing, mingling, and chemical equilibration. Chemie der Erde-Geochemistry 69, 247–277.
Kaygusuz, A., Aydınçakır, E., 2011. U–Pb zircon SHRIMP ages, geochemical and Sr–Nd isotopic compositions of Cretaceous plutons in the eastern Pontides (NE Turkey): the Dağbaşı pluton. Neues Jahrbuch Für Mineralogie 188 (3), 211–233.
Kaygusuz, A., Siebel, W., Şen, C., Satir, M., 2008. Petrochemistry and petrology of I-type granitoids in an arc setting: the composite Torul pluton, Eastern Pontides, NE Turkey. International Journal of Earth Sciences 97, 739–764.
Kaygusuz, A., Arslan, M., Siebel, W., Şen, C., 2011. Geochemical and Sr–Nd isotopic characteristics of post-collision calc-alkaline volcanics in the eastern Pontides (NE Turkey). Turkish Journal of Earth Sciences 20, 137–159.
Kaygusuz, A., Arslan, M., Siebel, W., Sipahi, F., Ilbeyli, N., 2012. Geochronological evidence and tectonic significance of Carboniferous magmatism in southwest Trabzon area, eastern Pontides, Turkey. International Geology Review 54, 1776–1800.
Keskin, M., Genç, Ş.C., Tüysüz, O., 2008. Petrology and geochemistry of post-collisional Middle Eocene volcanic units in North-Central Turkey: evidence for magma generation by slab breakoff following the closure of the Northern Neotethys Ocean. Lithos 104, 267–305.
Lambert, R.J., Holland, J.G., 1974. Yttrium geochemistry applied to petrogenesis utilizing calcium–yttrium relationships in minerals and rocks. Geochimica et Cosmochimica Acta 38, 1393–1414.
Le Bas, M.J., Le Maitre, R.W., Streckeisen, A., Zanettin, B., 1986. A chemical classification of volcanic rocks on the total alkali–silica diagram. Journal of Petrology 24 (3), 745–750.
Le Maitre, R.W., 2002. Igneous rocks: a classification and glossary of terms: recommendations of the International Union of Geological Sciences Subcommission on the Systematics of Igneous Rocks. Cambridge University Press, Cambridge 236 pp.
Le Roex, A.P., 1987. Source regions of mid-ocean ridge basalts; evidence for enrichment processes. In: Menzies, A.M., Hawkesworth, C.J. (Eds.), Mantle Metasomatism. Academic Press, London, pp. 389–422.
Leake, E.B., Wooley, A.R., Arps, C.E.S., Birch, W.D., Gilbert, M.C., Grice, J.D., Hawthorne, F.C., Kato, A., Kisch, H.J., Krivovichev, V.G., Linthout, K., Laird, J., Mandarino, J., Maresch, W.V., Nickhel, E.H., Rock, N.M.S., Schumacher, J.C., Smith, D.C., Stephenson, N.C.N., Ungaretti, L., Whittaker, E.J.W., Youzhi, G., 1997. Nomenc1ature of amphiboles report of the subcommittee on amphiboles of the International Mineralogical Association Commission on New Minerals and Mineral Names. European Journal of Mineralogy 9, 623–651.
McCulloch, M.T., Kyser, T.K., Woodhead, J.D., Kinsley, L., 1994. Pb–Sr–Nd–O isotopic constraints on the origin of rhyolites from the Taupo Volcanic Zone of New Zealand: evidence for assimilation followed by fractionation of basalt. Contributions to Mineralogy and Petrology 115, 303–312.
Morimoto, M., 1988. Nomenclature pyroxenes. Mineralogical Magazine 52, 535–550.
MTA, 2002. 1:500,000-scale map of Turkey, General Directorate of Mineral Research and Exploration (MTA), Ankara, Turkey.
Münker, C., Wörner, G., Yogodzinski, G., Churikova, T., 2004. Behaviour of high field strength elements in subduction zones: constraints from Kamchatka–Aleutian arc lavas. Earth and Planetary Science Letters 224, 275–293.
Nielsen, R.L., Forsythe, L.M., Gallahan, W.E., Fisk, M.R., 1994. Major- and trace element magnetite-melt equilibria. Chemical Geology 117, 167–191.
Nomade, S., Renne, T.P.R., Vogel, N., Deino, A.L., Sharp, W.D., Becker, T.A., Jaouni, A.R., Mundil, R., 2005. Alder Creek sanidine (Acs-2): a Quaternary $^{40}Ar/^{39}Ar$ dating standard tied to the Cobb Mountain geomagnetic event. Chemical Geology 218, 315–338.
Okay, A.I., 1996. Granulite facies gneisses from the Pulur Region, Eastern Pontides. Turkish Journal of Earth Sciences 5, 55–61.
Okay, A.I., Leven, E.J., 1996. Stratigraphy and paleontology of the upper Paleozoic sequences in the Pulur (Bayburt) region, Eastern Pontides. Turkish Journal of Earth Sciences 5, 145–155.
Okay, A.I., Şahintürk, Ö., 1997. Geology of the Eastern Pontides. In: Robinson, A.G. (Ed.), Regional and Petroleum Geology of the Black Sea and Surrounding Region: American Association of Petroleum Geologists (AAPG) Memoir, 68, pp. 291–311.
Okay, A., Tüysüz, O., 1999. Tethyan sutures of northern Turkey. In: Durand, B., Jolivet, L., Horvath, F., Serane, M. (Eds.), The Mediterranean Basins: Tertiary Extension within the Alpine Orogen: Geological Society, London, Special Publications, 156, pp. 475–515.
Pearce, J.A., 1983. Role of the sub-continental lithosphere in magma genesis at active continental margins. In: Hawkesworth, C.J., Norry, M.J. (Eds.), Continental Basalts and Mantle Xenoliths, Shiva, Cheshire, pp. 230–249.
Pearce, J.A., Norry, M.L., 1979. Petrogenetic implications of Ti, Zr, Y, and Nb variations in volcanic rocks. Contributions to Mineralogy and Petrology 69, 33–47.
Pearce, J.A., Bender, J.F., De Long, S.E., Kidd, W.S.F., Low, P.J., Güner, Y., Şaroğlu, F., Yılmaz, Y., Moorbath, S., Mitchell, J.J., 1990. Genesis of collision volcanism in eastern Anatolia Turkey. Journal of Volcanology and Geothermal Research 44, 189–229.
Qiao, G., 1988. Normalization of isotopic dilution analyses—a new program for isotope mass spectrometric analysis. Scientia Sinica 31, 1263–1268.
Ramezani, J., Tucker, R.D., 2003. The Saghand region, central Iran: U–Pb geochronology, petrogenesis and implications for Gondwana tectonics. American Journal of Science 303, 622–665.
Ringwood, A.E., 1990. Slab-mantle interactions: 3. Petrogenesis of intraplate magmas and structure of the upper mantle. Chemical Geology 82, 187–207.
Robertson, A.H.F., Ustaömer, T., Parlak, O., Ünlügenç, Ü.C., Taslı, K., Inan, N., 2006. The Berit transect of the Tauride thrust belt, S Turkey: late Cretaceous–early Cenozoic accretionary/collisional processes related to closure of the Southern Neotethys. Journal of Asian Earth Sciences 27, 108–145.
Robertson, A.H.F., Parlak, O., Rızaoğlu, T., Ünlügenç, Ü.C., Inan, N., Taslı, K., Ustaömer, T., 2007. Tectonic evolution of the South Tethyan ocean: evidence from the Eastern Taurus Mountains (Elazığ region, SE Turkey). Geological Society London Special Publications 272, 231–270.
Robinson, A.G., Banks, C.J., Rutherford, M.M., Hirst, J.P.P., 1995. Stratigraphic and structural development of the eastern Pontides, Turkey. Geological Society of London 152, 861–872.
Schmidberger, S.S., Hegner, E., 1999. Geochemistry and isotope systematics of calc-alkaline volcanic rocks from the Saar-Nahe basin (SW German)—implications for Late Variscan orogenic development. Contributions to Mineralogy and Petrology 135, 373–385.
Şen, C., 2007. Jurassic volcanism in the eastern Pontides: is it rift related or subduction related? Turkish Journal of Earth Sciences 16, 523–539.
Şen, C., Arslan, M., Van, A., 1998. Doğu Pontid (Kd Türkiye) Eosen (?) Alkalen Volkanik Provensinin Jeokimyasal ve Petrolojik Karakteristikleri, Tübitak Yayinlari. Turkish Journal of Earth Sciences 7, 231–239.
Şengör, A.M.C., Yılmaz, Y., 1981. Tethyan evolution of Turkey: a plate tectonic approach. Tectonophysics 75, 181–241.
Şengör, A.M.C., Yılmaz, Y., Ketin, I., 1980. Remnants of pre–late Jurassic ocean in northern Turkey: fragments of Permian–Triassic Paleo-Tethys. Geological Society of America Bulletin 91, 599–609.
Şengör, A.M.C., Özeren, S., Genç, T., Zor, E., 2003. East Anatolian high plateau as a mantle-supported, North–south shortened domal structure. Geophysical Research Letters 30 (24), 8045. http://dx.doi.org/10.1029/2003gl017858.
Smith, E.I., Sanchez, A., Walker, J.D., Wang, K., 1999. Geochemistry of mafic magmas in the Hurricane Volcanic field, Utah: implications for small and large scale chemical variability of the lithosheric mantle. Journal of Geology 107, 433–448.
Staudigel, H., Davies, G.R., Hart, S.R., Marchant, K.M., Smith, B.M., 1995. Large scale isotopic Sr, Nd and O isotope anatomy of altered oceanic crust at DSDP7ODP sites 417/418. Earth and Planetary Science Letters 130, 169–185.
Stöcklin, J., 1971. Stratigraphic lexicon of Iran. Part 1: Central, North and East Iran. Geological Survey of Iran. (338 pp.).
Sun, S., McDonough, W.F., 1989. Chemical and isotopic systematics of oceanic basalt: implications for mantle composition and processes. In: Saunders, A.D., Norry, M.J. (Eds.), Magmatism in the Ocean Basins: Geological Society of London Special Publication, 42, pp. 313–345.
Tatsumi, Y., Eggins, S.M., 1995. Subduction Zone Magmatism. Blackwell, Cambridge (211 pp.).
Taylor, S.R., McLennan, S.M., 1985. The Continental Crust, Its Composition and Evolution. Blackwell, Oxford 312 pp.
Temizel, İ., Arslan, M., 2005. Mineral chemistry and petrochemistry of Tertiary calc-alkaline volcanic rocks in the İkizce (Ordu) area, NE Turkey. Earth Sciences 26 (1), 25–47.
Temizel, İ., Arslan, M., 2008. Petrology and geochemistry of Tertiary volcanic rocks from the İkizce (Ordu) area, NE Turkey: implications for the evolution of the eastern Pontide paleo-magmatic arc. Journal of Asian Earth Sciences 31 (4–6), 439–463.
Temizel, İ., Arslan, M., 2009. Mineral chemistry and petrochemistry of post-collisional Tertiary mafic to felsic cogenetic volcanics in the Ulubey (Ordu) area, eastern Pontides, NE Turkey. Turkish Journal of Earth Sciences 18, 29–53.
Temizel, İ., Arslan, M., Ruffet, G., Peucat, J.J., 2012. Petrochemistry, geochronology and Sr–Nd isotopic systematic of the Tertiary collisional and post-collisional volcanic rocks from the Ulubey (Ordu) area, eastern Pontide, NE Turkey: implications for extension-related origin and mantle source characteristics. Lithos 128, 126–147.
Thirlwall, M.F., Smith, T.E., Graham, A.M., Theodorou, N., Hollings, P., Davidson, J.P., Arculus, R.J., 1994. High field strength element anomalies in arc lavas; source or process? Journal of Petrology 35 (3), 819–838.
Thirlwall, M.F., Graham, A.M., Arculus, R.J., Harmon, R.S., Macpherson, C.G., 1996. Resolution of the effects of crustal assimilation, sediment subduction, and fluid transport in island arc magmas: Pb–Sr–Nd–O isotope geochemistry of Grenada, Lesser Antilles. Geochimica et Cosmochimica Acta 60, 4785–4810.
Thompson, R.N., Morrison, M.A., Hendry, G.L., Parry, S.J., 1984. An assessment of the relative roles of crust and mantle in magma genesis: an elemental approach. Philosophical Transactions of the Royal Society 310, 549–590.
Tokel, S., 1977. Doğu Karadeniz Bölgesi'nde Eosen Yaşlı Kalkalkalen Andezitler ve Jeotektonizma. Türkiye Jeoloji Kurumu Bülteni 20, 49–54.
Topuz, G., Altherr, R., Schwarz, W.H., Siebel, W., Satir, M., Dokuz, A., 2005. Postcollisional plutonism with adakite-like signatures: the Eocene Saraycik granodiorite (Eastern Pontides, Turkey). Contributions to Mineralogy and Petrology 150, 441–455.
Topuz, G., Altherr, R., Schwarz, W.H., Dokuz, A., Meyer, H.P., 2007. Variscan amphibolite-facies rocks from the Kurtoğlu metamorphic complex. Gümüşhane area, Eastern Pontides, Turkey. International Journal of Earth Sciences 96, 861–873.
Topuz, G., Altherr, R., Wolfgang, S., Schwarz, W.H., Zack, T., Hasanözbek, A., Mathias, B., Satır, M., Şen, C., 2010. Carboniferous high-potassium I-type granitoid magmatism in the Eastern Pontides: the Gümüşhane pluton (NE Turkey). Lithos 116, 92–110.

Topuz, G., Okay, A.I., Altherr, R., Schwarz, W.H., Siebel, W., Zack, T., Satir, M., Şen, C., 2011. Post-collisional adakite-like magmatism in the Ağvanis massif and implications for the evolution of the Eocene magmatism in the Eastern Pontides (NE Turkey). Lithos 125, 131–150.

Tribuzio, R., Tiepolo, M., Vannucci, R., Bottazzi, P., 1999. Trace element distribution within olivine-bearing gabbros from the Northern Apennine ophiolites (Italy): evidence for post-cumulus crystallization in MOR-type gabbroic rocks. Contributions to Mineralogy and Petrology 134, 123–133.

Ustaömer, T., Robertson, H.F.A., 2010. Late Paleozoic–Early Cenozoic development of the Eastern Pontides (Artvin area), Turkey: stages of closure of Tethys along the southern margin of Eurasia. Special Publications, Geological Society London 340, 281–327.

Vincent, S.J., Allen, M.B., Ismail-Zadeh, A.D., Flecker, R., Foland, K.A., Simmons, M.D., 2005. Insights from the Talysh of Azerbaijan into the Paleogene evolution of the South Caspian region. Geological Society of America Bulletin 117, 1513–1533.

Wilson, M., 1989. Igneous Petrogenesis. Oxford University Press, Oxford (466 pp.).

Winchester, J., Floyd, P.A., 1977. Geochemical discrimination of different magma series and their differentiation products using immobile elements. Chemical Geology 20, 325–343.

Yiğitbaş, E., Yılmaz, Y., 1996. New evidence and solution to the Maden complex controversy of the Southeast Anatolian orogenic belt (Turkey). Geologische Rundcshau 85, 250–263.

Yılmaz, Y., 1972. Petrology and Structure of the Gümüşhane Granite and the Surrounding Rocks. NE Anatolia. PhD Thesis University College London, England (248 pp.).

Yılmaz, S., Boztuğ, D., 1996. Space and time relations of three plutonic phases in the Eastern Pontides, Turkey. International Geology Review 38, 935–956.

Yılmaz, A., Engin, T., Adamia, S., Lazarashvili, T., 1997. Geoscientific Studies of the Area Along Turkish–Georgian Border. MTA, Ankara.

Yılmaz, A., Adamia, S., Chabukiani, A., Chkhotua, T., Erdoğan, K., Tuzcu, S., Karabıyıkoğlu, M.F., 2000. Structural correlation of the southern Transcaucasus (Georgia)–eastern Pontides (Turkey). In: Bozkurt, E., Winchester, J.A., Piper, J.D.A. (Eds.), Tectonics and Magmatism in Turkey and the Surrounding Area: Geological Society London Special Publications, 173, pp. 171–182.

Zhang, H.-F., Sun, M., Zhou, X., Fan, W.M., Yın, J.F., 2002. Mesozoic lithosphere destruction beneath the North China Craton: evidence from major, trace element, and Sr–Nd–Pb isotope studies of Fangcheng Basalts. Contributions to Mineralogy and Petrology 144, 241–253.